Electromagnetic response of a pinned Wigner crystal

H. A. Fertig
Department of Physics and Astronomy, University of Kentucky, Lexington, Kentucky 40506-0055
(Received 18 September 1997; revised manuscript received 22 December 1997)

A microscopic model for analyzing the microwave absorption properties of a pinned, two-dimensional Wigner crystal in a strong perpendicular magnetic field is developed. The method focuses on excitations within the lowest Landau level, and corresponds to a quantum version of the harmonic approximation. For pure systems (no disorder), the method reproduces known results for the collective mode density of states of this system, and clearly identifies the origin of previously unexplained structure in this quantity. The application of the method to a simple diagonal disorder model uncovers a surprising result: a sharp (δ-function) response at zero temperature that is consistent with recent experiments. A simple spin lattice model is developed that reproduces the results of the quantum harmonic approximation, and shows that the sharp response is possible because the size scale L_c of patches moving together in the lowest-frequency collective mode is extremely large compared to the sample size for physically relevant parameters. This result is found to be a direct repercussion of the long-range nature of the Coulomb interaction. Finally, the model is used to analyze different disorder potentials that may pin the Wigner crystal, and it is argued that interface disorder is likely to represent the dominant pinning source for the system. A simple model of the interface is shown to reproduce some of the experimental trends for the magnetic field dependence of the pinning resonance.
[S0163-1829(99)07703-6]

I. INTRODUCTION

It has long been appreciated that the ground state of electrons in an otherwise structureless environment should be crystalline at low enough densities.[1] Considerable effort has been focused on creating such a state in a two-dimensional electron gas (2DEG) as realized in semiconductor heterojunction and quantum well systems,[2] although obtaining the appropriate limit of low electron and impurity densities has proven difficult. The introduction of a magnetic field perpendicular to the 2DEG improves this situation by raising the electron density at which crystallization is thought to occur. Recent experiments have identified the onset of strong insulating behavior in very high mobility systems, at magnetic fields such that the filling factor $\nu = N/N_\phi$, with N the number of electrons and N_ϕ the number of magnetic flux quanta through the system, is below $\sim 1/5$ for electrons[3,4] and $\sim 1/3$ for hole systems.[5] While much intriguing experimental data has accumulated, a definitive proof that the low filling factor insulating state of these two-dimensional systems is indeed an electron, or Wigner, crystal (WC) has remained elusive.

One experimental fact for the low filling factor systems that is in clear agreement with expectations for a WC interpretation is that they are insulating. It is well appreciated by now, from analogous behavior in charge density wave (CDW) systems,[6] that an arbitrarily small disorder potential should pin the WC at zero temperature so that there are no charge carriers that can flow in response to an arbitrarily small static electric field. In CDW systems, the pinning potential also supplies a restoring force that induces a broad peak in the ac electromagnetic response at the ''pinning frequency,'' whose magnitude may be used to assess the correlation length of the CDW.[6,7] Early experiments on the magnetically-induced WC identified similar structure in the density response using various techniques.[8–11] Theoretical analyses[12–14] of these experiments have largely focused on determining the correlation length of the WC from the experimental data, although no clear consensus on this quantity has yet been reached.

Very recently, experiments on high-quality hole[15,16] and electron[17] systems at low filling factors have revealed structures in their microwave absorption properties that are *qualitatively different* than what is observed in CDW systems. At the lowest temperatures and highest magnetic fields available, these systems exhibit *sharp* resonances at low frequencies, with quality factors $Q = f/\Delta f$ (f here is the frequency of the resonance peak and Δf its width) as high as 30. The frequency of the peak increases with increasing magnetic field, and may saturate at a maximum for the largest fields.[15] By contrast, most existing theoretical work predicts[12,13,18,19] a broad ($Q \sim 1$) resonance, and a pinning frequency that *decreases* with magnetic field. The subject of this work is to understand some aspects of this puzzling experimental finding.

In what follows we will adopt a microscopic model of the magnetically induced two-dimensional Wigner crystal. The ground state is assumed to be well described by a product of localized Gaussian wave packets, so that exchange effects are ignored.[20] Our goal is to find the response of the system to a time-dependent, spatially uniform electric field.[21] To compute the latter quantity we will employ a ''quantum harmonic approximation'' (QHA),[22] a natural generalization of the classical harmonic approximation, in which a finite number of angular momentum orbitals per site is retained in the Hilbert space of states for the electron system. This is, of course, sensible provided that the electrons remain close to their ground state sites after being excited by the electric field. A very strong magnetic field is assumed so that projection into the lowest Landau level is appropriate,[23] and all

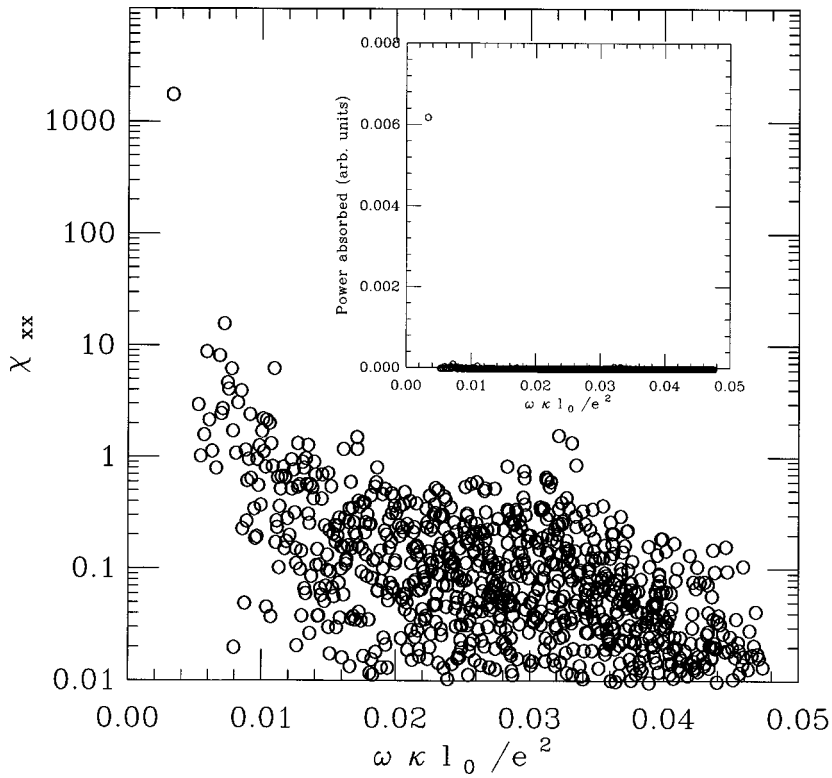

FIG. 1. Center of mass response function $\chi^{xx}_{\text{c.m.}}$ for a system of $N=1024$ electrons at $\nu=0.2$. Half the sites are chosen at random to have a pinning potential $\Delta U_i=0.01e^2/\kappa l_0$ (see text); the other half are unpinned. Two states per site were retained in this calculation (see text). Inset: Relative power absorption for the same system.

results reported here are for zero temperature. For an undisordered WC, the QHA reproduces known results found *without* resorting to a harmonic approximation,[24] and indeed offers an explanation of features found in the density response function that were not easily interpreted previously.

Because exchange effects are negligible in this system,[20] a time-dependent Hartree approximation turns out to be both convenient and accurate for computing the response functions of this system. For simplicity we consider only a diagonal disorder model; i.e., the disorder enters only in the single particle excitation energies and not in the interaction matrix elements among the electrons. In practice this means we have adopted a model in which the lattice is perfectly ordered, and disorder is introduced as a random on-site pinning potential.[25] As we will see, this assumption greatly simplifies the computation of matrix elements entering the QHA. Using a perturbative approach described below, for weak disorder it is possible to demonstrate that our qualitative results are insensitive to the diagonal disorder assumption.

For all the disorder models studied in this work, the results of the QHA turn out to be qualitatively the same: the response functions exhibit an extremely sharp response at the lowest collective mode frequency (provided that the electron-electron interaction is unscreened; see below.) This is the central result of this work. Two physical models of pinning are analyzed in detail in this study. Charged impurities which may be found in the spacer layer between donors and the electrons have been argued[26] to represent the strongest source of pinning for the WC in dc nonlinear I-V measurements; i.e., these set the energy scale necessary to fully dislodge the electrons in a nonvanishing static electric field so that a current may flow. From the CDW point of view,[7] this model corresponds to a strongly pinned system. However, we will see that the strong pinning approach grossly overestimates the pinning frequency, so that the experimentally measured pinning frequencies cannot be explained by this source of disorder.[27] The ultimate reason for the discrepancy between the pinning frequency in the microscopic model and the CDW result for this is that a magnetically induced WC is *not* a CDW. Our results indicate that the collective mode spectrum associated with strongly pinned centers is far more like that of a crystal with vacancies pinned at charged impurity sites than that of an elastic medium tied down at random sites.

We then focus on a model of interface disorder that we believe is likely to be the dominant pinning mechanism in electromagnetic absorption for these systems. Heterostructure and quantum well interfaces are believed to have structure at length scales of several tens of angstroms.[28] An interpretation of this is that in semiconductor heterostructures the interface between different materials (typically GaAs and AlAs) may only be defined to within one or two lattice constants (~ 5 Å). This is often modeled as an interface with pits and/or islands of typical size scale <100 Å.[29] Electrons residing in large pits or regions with an unusually large number of small pits have an enhanced probability of lying slightly closer to the donor layer and so may be bound by them. An important aspect of the physics in this model is that in the lowest Landau level interfaces with pits whose size scales are smaller than the magnetic length $l_0=(\hbar c/eB)^{1/2}$ have pinning potentials that increase with decreasing l_0. This leads to an *increasing* pinning frequency with magnetic

field, as seen in experiment. The ~ 1 GHz magnitude of the measured pinning frequency may be explained with very reasonable parameters describing the interface at which the 2DEG resides, as described below.

A typical result for a single disorder realization, whose precise form is described below, is shown in Fig. 1. The system includes 1024 electrons, and is assumed here (as throughout this work) to obey periodic boundary conditions. Because of the finite number of degrees of freedom, the density response function consists of a series of δ functions. Note that the scale of the figure is logarithmic, so that a linear plot of power absorbed as a function of frequency shows a single δ-function response at the lowest collective mode frequency, as illustrated in the inset. The height of this peak shows no sign of decreasing with increasing system size, nor do any other collective modes develop a noticeable oscillator strength in power absorption. For a model in which the typical on-site pinning potential is small, we find the pinning frequency (i.e., the position of the δ-function response in Fig. 1) to a good approximation is given by v_0, the energy required to excite an electron from the $m=0$ to the $m=1$ angular momentum state in the absence of other electrons, averaged over all the electrons. This value is essentially the same as the well-known result for weakly pinned CDW's.[7] Typically, the exact pinning frequency found in the QHA falls somewhat below this estimate, by an amount that is specific to the precise disorder realization. This correction to the weak pinning result may be estimated using a perturbative approach described below.

Although the sharpness of the absorption peak seems to be in agreement with recent experiments, one needs some analytic method to demonstrate that in the thermodynamic limit the peak does not broaden, particularly since this result is so different from prior expectations.[13,18] Towards this end we develop a (pseudo)spin lattice model in which the $\hat{z}$ component of the spin at a given site represents the angular momentum state of an electron. A convenient perturbation theory for the system may be developed around a uniformly pinned state (i.e., one in which the pinning potential for every site is v_0). The perturbing parameter is then $\Delta U(\vec{R})$, with $\{\vec{R}\}$ representing the sites around which the electrons are localized and $U(\vec{R})=v_0+\Delta U(\vec{R})$ is the energy required to excite an electron from the $m=0$ to the $m=1$ state. For the uniformly pinned system, it is natural for the power absorbed to have a δ-function response, since the collective modes have wave vector $\vec{q}$ as a good quantum number. The correction to the weight W of this δ function due to disorder may be computed in perturbation theory, and a depletion D may be defined such that $W \propto 1-D$. To lowest nontrivial order in perturbation theory, the largest contribution to D is found to have the form

$$D \propto \int d^2q \frac{|\Delta U(\vec{q})|^2 |u_{\vec{q}}^+|^2}{|E_{\vec{q}}^p - E_{q=0}^p|^2}. \tag{1}$$

Here $\vec{q}$ represents wave vector, $\Delta U(\vec{q})$ the Fourier transform of the perturbation, and $E_{\vec{q}}^p$ the collective mode dispersion for the uniformly pinned system. $|u_{\vec{q}}^+|^2$ is a weighting function whose precise form is given below; in the limit $q \to 0$, $|u_{\vec{q}}^+| \to 1$. Provided that the disorder potential does not have fluctuations on arbitrarily long length scales — i.e., that arbitrarily large patches of unpinned or strongly pinned electrons are rare — then one expects $|\Delta U(\vec{q})|^2 \propto q^2$ for small q. The dispersion relation for the uniformly pinned system we show below has the form

$$E_{\vec{q}}^p \approx v_0 + 2\pi e^2 \rho_0 l_o^2 q/\kappa + O(q^2) \tag{2}$$

for small q, where ρ_0 is the electron density and κ is the dielectric constant of the host semiconductor. The linear dispersion with q turns out to be a direct result of the long-range nature of the Coulomb interaction, and is not present in a model with short-range (e.g., screened) electron-electron interactions. Plugging Eq. (2) into Eq. (1) demonstrates that for a given disorder realization a finite depletion results that will be small if the pinning is not too far from uniform. This directly demonstrates that it is the long-range nature of the electron-electron interaction that is responsible for the sharp response in the system. A system with short-range interactions has a collective mode spectrum dispersing *quadratically* with q away from v_0, and as seen for Eq. (1), this leads to a divergence in D, signaling that the response is *not* sharp in this case. Figure 2 illustrates the response function for a model in which the electron-electron interaction is screened. As may be seen, even for a relatively small number of particles ($N=225$), the response has been significantly broadened, as is typically found in CDW systems.[6,7,13] Roughly speaking, this says that an appropriate analogy for the randomly pinned WC in a strong magnetic field is a hard object that does not deform much when vibrating on randomly placed springs, so that a well-defined periodic response is to be expected in spite of the randomness of the pinning.

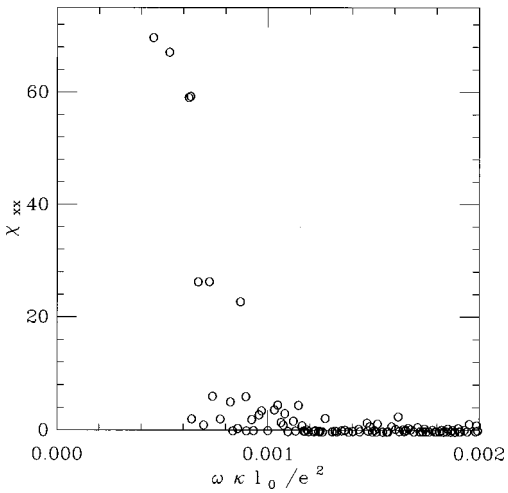

FIG. 2. Center of mass response function $\chi_{\text{c.m.}}^{xx}$ for a system of size $N=225$ electrons at $\nu=0.2$ with a screened Coulomb potential of the form $v(q)=2\pi e^2/\kappa(q^2+q_c^2)^{1/2}$, with $q_c=2.0/l_0$. Half the sites are chosen at random to have a pinning potential $\Delta U_i = 0.01 e^2/\kappa l_0$ (see text); the other half are unpinned. Two states per site were retained in this calculation. The result indicates that screening broadens the response, so that the sharpness of the response illustrated in Fig. 1 is related to the long-range nature of the Coulomb interaction.

One important caveat to this result must be noted. The assumption that $|\Delta U(\vec{q})|^2 \propto q^2$ is actually not true for the most common forms of disorder studied. Specifically, white-noise pinning models usually have equal fluctuation strengths at all length scales, so that ΔU does not vanish as $q \to 0$. In our expression, Eq. (1), this leads to a formal logarithmic divergence in the thermodynamic limit and an expected broadening of the absorption peak. We note, however, that the disorder models used in the QHA have a white-noise character, yet we have not been able to detect a finite width in the resonance for any disorder realization. Presumably this indicates that the δ-function response is a finite system size effect, and one needs to estimate a length scale above which broadening in the response function should become apparent. This may be accomplished by noting that the integral in Eq. (1) has an infrared cutoff $2\pi/L$ where L is the system size. The value of L for which $D \approx 1$, which we call L_c, sets the size scale above which broadening will be significant. Solving for L_c, one finds

$$L_c \approx \ell \exp\left\{ \frac{\nu^3}{|\Delta \tilde{U}|^2} \right\},$$

where ℓ is a length scale above which Eq. (2) is accurate ($\ell \approx 10 a_0$, with a_0 the WC lattice constant), and $\Delta \tilde{U} = \lim_{q \to 0} \Delta U(\vec{q}) \kappa l_0 / e^2$.

The physical interpretation of L_c is that it is the length scale for coherent motion of patches of electrons in the lowest collective mode, since for $L \ll L_c$ the perturbation theory is valid and the system responds much like a single oscillator to the excitation field. A conservative estimate of L_c for the experiments of Refs. 15 and 16 shows that in practice it is huge, $L_c > 10^{24} a_0$ at $\nu = 0.22$, where a_0 is the lattice constant of the WC. Thus, remarkably, in spite of the formal divergence in the thermodynamic limit, the perturbation theory is in fact controlled and valid for samples with physically relevant dimensions, where $L \sim 10^5 a_0 \ll L_c$. Thus our interpretation of the WC response as one of an undeformable oscillator is indeed appropriate.

This article is organized as follows. In Sec. II we develop the QHA used to compute the electromagnetic response of the pinned WC. Section III develops the pseudospin approach to the collective modes and shows how a perturbation theory may be developed around the uniformly pinned state, and the calculation of the depletion D is discussed. Section IV discusses some details of the interface pinning model. Readers interested in our results and not the details of the calculations may wish to proceed directly to Sec. V, which discusses results for different pinning models, including charged impurities in the electron layer and the interface pinning model. Section VI discusses the relationship of this work with results of other calculations, as well as several unresolved questions regarding the experimental results. We conclude with a summary in Sec. VII.

II. QUANTUM HARMONIC APPROXIMATION

In this section we will develop a quantum mechanical generalization of the harmonic approximation, in which the electrons are treated as distinguishable, so that the ground state and low-lying excited states may be represented as linear combinations of (unsymmetrized) products of single particle states. The single particle states we will use consist of angular momentum states, and we will find that it is an excellent approximation to retain only the lowest-lying ones when computing low-energy properties of the system. Once we have truncated the Hilbert space in this way, it becomes possible to numerically compute response functions for reasonably large systems, which one may compare with experiment.

The ground state of two-dimensional charged particles in a very strong magnetic field is believed[20] to be accurately represented by a collection of distinguishable particles in Gaussian orbitals of the form

$$\phi_{0,\vec{R}_i}(\vec{r}_i) = \left(\frac{1}{2\pi l_0^2} \right)^{1/2} e^{-|\vec{r}_i - \vec{R}_i|^2/4l_0^2 + (i/2)\hat{z}\cdot(\vec{R}_i \times \vec{r}_i)/l_0^2}.$$

In this state, the electron with coordinate $\vec{r}_i$ is maximally localized within the lowest Landau level. Since the kinetic energy of a collection of electrons in such orbitals is already as small as possible, the ground state presumably will be found by minimizing the total potential energy with respect to the parameters $\vec{R}_i$. In the absence of disorder these should be chosen to lie on a perfect lattice, so that the charge distribution in the limit of infinite magnetic field ($l_0 \to 0$) approaches that of the ground state for a distribution of *classical* point particles. Disorder changes the optimal positions for the electrons,[30] but provided the disorder is not too strong, the site centers $\vec{R}_i$ will presumably not be close to one another on the scale of the magnetic length l_0. In this situation, wave function overlaps among the individual electrons are negligible, so that a product of the single particle wave packets $\phi_{0,\vec{R}_i}(\vec{r}_i)$ is an accurate representation of the ground state, despite the fact that it is not explicitly antisymmetric.[20]

Since we are interested in the electromagnetic response of the system at low frequencies, it will be necessary to compute the low-lying excited states of the system. In a classical analysis, this is typically done by assuming the displacements of the electrons from their ground state positions are small, so that the energy may be expanded to second order in displacements, allowing the normal modes of the system to be found in a relatively simple fashion. If we assume the electrons are localized within a magnetic length of their ground state positions, then the analog of the small displacements approximation is to allow individual electrons to be excited into higher angular momentum states localized about each lattice site. Provided the angular momentum is not too large, the charge densities associated with these states for a given site will not overlap significantly with those of its neighbors, so that exchange effects may continue to be ignored. Thus we consider a set of states for each site

$$\phi_{m,i}(\vec{r}) = \left(\frac{1}{2\pi l_0^2 2^m m!} \right)^{1/2} \left(\frac{z - Z_i}{l_0} \right)^m \times e^{-|\vec{r} - \vec{R}_i|^2/4l_0^2 + (i/2)\hat{z}\cdot(\vec{R}_i \times \vec{r})/l_0^2}, \quad (3)$$

where $z = x + iy$ is the electron position in complex notation, and $Z_i = R_i^x + iR_i^y$. If we define creation operators for these

single particle states $a^{\dagger}_{mi}$, then the Hamiltonian for the system may approximately be written in the form

$$H=\sum_i \sum_{mn} V^i_{mn} a^{\dagger}_{mi} a_{ni} + \frac{1}{2}\sum_{i\neq j}\sum_{m_i n_i m_j n_j} U^{ij}_{m_i n_i m_j n_j} a^{\dagger}_{m_i i} a_{n_i i} a^{\dagger}_{m_j j} a_{n_j j}.$$

Here, V^i_{mn} represents the interaction of an isolated electron with a disorder potential, and the interaction matrix element is given by

$$U^{ij}_{m_1 m_2 m_3 m_4} = \int d^2 r_1 d^2 r_2 \left(\frac{1}{2\pi l_0^2}\right)^2 \times \left[\frac{1}{2l_0^2}\right]^{(m_1+m_2+m_3+m_4)/2} \times z_1^{*m_1} z_1^{m_2} z_2^{*m_3} z_2^{m_4} e^{-r_1^2/2l_0^2 - r_2^2/2l_0^2} \times v(\vec{r}_1 - \vec{r}_2 + \vec{R}_{ij}), \quad (4)$$

where for most cases we will study, $v(r)$ is the Coulomb interaction $e^2/\kappa r$, with κ the dielectric constant of the host material for the electron layer.

To simplify our calculations, we will make certain assumptions about the form of the disorder entering H. First, we assume that although disorder certainly will cause the orbit centers $\vec{R}_i$ to vary from the positions of a perfect lattice, this variation does not affect the qualitative features of the absorption spectrum. Thus in practice our $\vec{R}_i$'s take on the values of perfect triangular lattice positions. It should be noted that this choice of the $\vec{R}_i$'s is not required to carry out the QHA, but by adopting it the numerical computation of $U^{ij}_{m_i n_i m_j n_j}$ is greatly simplified. Some details on how this is done in practice are discussed in the Appendix. The second simplification we introduce is to assume that the pinning potential at the individual sites is circularly symmetric, so that in the ground state the electrons occupy the $\phi_{m=0,i}$ orbitals and do not admix higher angular momentum states. Again, the QHA may be developed without this assumption. However, this simplification has the great advantage of allowing an analytic specification of the ground state. In the absence of this assumption one would need to find the ground state orbital occupations numerically, which presumably could be computed with sufficient accuracy using a static Hartree approximation. While such a calculation is clearly feasible, we believe that allowing asymmetric forms for V^i_{mn} will have little quantitative effect, provided the average of this quantity over the sites restores the circular symmetry. Finally, to take full advantage of the symmetries of the system, we will impose periodic boundary conditions.

A second caveat related to this is that in principle one must retain fewer than seven orbitals on each site to have each electron lie purely in the $m=0$ orbital in the ground state. Even in the absence of disorder, the sixfold symmetry of the lattice will in principle admix in states with angular momenta equal to integral multiples of six. Although this effect is extremely small,[20] it can in principle lead to weak instabilities in the response function computed below when too many orbitals are included per site. As we will see, all the low-energy excitations (i.e., phonons) of the system are accurately captured when only *two* orbitals per site are retained, so that in practice this does not arise as a problem.

With these simplifications, the Hamiltonian takes the form

$$H=\sum_i \sum_m \varepsilon_i(m) a^{\dagger}_{mi} a_{mi} + \frac{1}{2}\sum_{i\neq j}\sum_{m_i n_i m_j n_j} U^{ij}_{m_i n_i m_j n_j} a^{\dagger}_{m_i i} a_{n_i i} a^{\dagger}_{m_j j} a_{n_j j}. \quad (5)$$

The zero of energy may always be chosen such that $\varepsilon_i(m=0)=0$, and we expect $\varepsilon_i(m>0)\geqslant 0$. The choice of $\{\varepsilon_i(m)\}$ defines the specific disorder model we are studying. We note that the greatest power of this method is that it is well suited to disorder potentials that vary on length scales of the order of l_0 and smaller. The two pinning mechanisms we study in detail — charged impurities and interface pinning — both fall into this category.

The quantity we will calculate, from which either power absorption or frequency-dependent conductivity may be computed, is the response function

$$\chi_{m_1 m_2 m_3 m_4}(ij;\tau) = -\langle T_\tau a^{\dagger}_{m_1 i}(\tau) a_{m_2 i}(\tau) a^{\dagger}_{m_3 j}(0) a_{m_4 i}(0)\rangle, \quad (6)$$

where here τ is imaginary time and $a_{mi}(\tau)$, $a^{\dagger}_{mi}(\tau)$ are the usual time-dependent Heisenberg representations of the annihilation and creation operators, and T_τ the time ordering operator.[31] The brackets $\langle\ \rangle$ represent a thermal average. The Fourier transform of this function with respect to imaginary time has poles at the collective mode frequencies. To generate a closed formula for χ, we employ an equation of motion method similar to that used in Ref. 24. The time derivative of χ satisfies the equation

$$\frac{\partial \chi_{m_1 m_2 m_3 m_4}(ij;\tau)}{\partial \tau} = -\langle[\rho_{m_1 m_2}(i;\tau), \rho_{m_3 m_4}(j;0)]\rangle \delta(\tau) - \left\langle T_\tau \frac{\partial \rho_{m_1 m_2}(i;\tau)}{\partial \tau} \rho_{m_3 m_4}(j;0)\right\rangle, \quad (7)$$

where $\rho_{m_1 m_2}(i;\tau) = a^{\dagger}_{m_1 i}(\tau) a_{m_2 i}(\tau)$. The time derivative of ρ may be computed from the Heisenberg equation of motion

$$\frac{\partial \rho_{m_1 m_2}(i;\tau)}{\partial \tau} = [H-\mu N, \rho_{m_1 m_2}(i;\tau)].$$

Note that the formal inclusion of the chemical potential μ is necessary because of the use of the finite temperature formalism; this means our formalism allows in principle for us to treat the situation in which there is more than one electron per site. In what follows, μ will be chosen such that there is one electron per site in the ground state, and we will see in

any case that any formal dependence on μ drops out of our equations for the response functions, so that it does not need to be explicitly computed. The relevant commutators in the equation of motion may be worked out using $\{a_{mi}, a_{nj}^{\dagger}\} = \delta_{mn}\delta_{ij}$ (Ref. 32) from which one may show

$$[\rho_{m_1m_2}(i), \rho_{m_3m_4}(j)] = [\rho_{m_1m_4}(i)\delta_{m_2m_3} - \rho_{m_3m_2}(i)\delta_{m_1m_4}]\delta_{ij}. \quad (8)$$

Combining Eqs. (5), (7), and (8), the equation of motion takes the form

$$\frac{\partial \chi_{m_1m_2m_3m_4}(ij;\tau)}{\partial \tau} = -[\langle \rho_{m_1m_4}(i)\rangle \delta_{m_2m_3} - \langle \rho_{m_3m_2}(i)\rangle \delta_{m_1m_4}]\delta_{ij}\delta(\tau) + [\varepsilon_i(m_1) - \varepsilon_i(m_2)]\chi_{m_1m_2m_3m_4}(ij;\tau) - \sum_{n_1n_2n_3n_4}\sum_{l} U'^{il}_{n_1n_2n_3n_4}\langle T_\tau[\rho_{n_1m_2}(i;\tau)\rho_{n_3n_4}(l;\tau)\delta_{n_2m_1} - \rho_{m_1n_2}(i;\tau)\rho_{n_3n_4}(l;\tau)\delta_{n_1m_2}]\rho_{m_3m_4}(j;0)\rangle. \quad (9)$$

Here $U'^{il}_{n_1n_2n_3n_4} = U^{il}_{n_1n_2n_3n_4}(1-\delta_{il})$. To obtain a closed form for the equation of motion, we utilize a Hartree decomposition of the last term in Eq. (9). This is very much in the spirit of Ref. 24; however, because we are ignoring overlap among single particle states located at different sites, it is unnecessary (and in fact would be inappropriate) to include exchange terms in the decomposition. We thus make the substitution

$$\begin{aligned}&[\rho_{n_1m_2}(i;\tau)\rho_{n_3n_4}(l;\tau)\delta_{n_2m_1} - \rho_{m_1n_2}(i;\tau)\rho_{n_3n_4}(l;\tau)\delta_{n_1m_2}]\\ &\quad\rightarrow [\rho_{n_1m_2}(i;\tau)\delta_{n_2m_1} - \rho_{m_1n_2}(i;\tau)\delta_{n_1m_2}]\langle \rho_{n_3n_4}(l)\rangle\\ &\qquad + [\langle \rho_{n_1m_2}(i)\rangle \delta_{n_2m_1} - \langle \rho_{m_1n_2}(i)\rangle \delta_{n_1m_2}]\rho_{n_3n_4}(l;\tau).\end{aligned}$$

Substituting the above decomposition and Fourier transforming Eq. (9) with respect to imaginary time, we arrive at the time-dependent Hartree approximation for the response function:

$$\begin{aligned}&i\omega_n\chi_{m_1m_2m_3m_4}(ij;i\omega_n)\\ &\quad = -[\langle \rho_{m_1m_4}(i)\rangle \delta_{m_2m_3} - \langle \rho_{m_3m_2}(i)\rangle \delta_{m_1m_4}]\delta_{ij}\\ &\qquad + [\varepsilon_i(m_1) - \varepsilon_i(m_2)]\chi_{m_1m_2m_3m_4}(ij;i\omega_n)\\ &\qquad + \sum_{n_1n_2n_3n_4}\sum_{l} U'^{il}_{n_1n_2n_3n_4}\{[\chi_{n_1m_2m_3m_4}(ij;i\omega_n)\delta_{n_2m_1}\\ &\qquad - \chi_{m_1n_2m_3m_4}(ij;i\omega_n)\delta_{n_1m_2}]\langle \rho_{n_3n_4}(l)\rangle\\ &\qquad + [\langle \rho_{n_1m_2}(i)\rangle \delta_{n_2m_1} - \langle \rho_{m_1n_2}(i)\rangle \delta_{n_1m_2}]\\ &\qquad \times \chi_{n_3n_4m_3m_4}(lj;i\omega_n)\}. \quad (10)\end{aligned}$$

Once we have solved Eq. (10), in principle we may compute any response function we like. However, since ultimately we are interested in the conductivity or power absorption of the system for a spatially uniform electric field, it is convenient to formulate the equation for a response function that is less cumbersome in terms of indices, but which may still be used to compute the physical quantities of interest. Towards this end we just consider the center of mass response of the system. An operator corresponding to the displacement of the center of mass may be written in the form

$$\vec{u}_{\text{c.m.}} = \frac{1}{N}\sum_{m_1m_2}\sum_{i}\langle m_1, i|\vec{r} - \vec{R}_i|m_2, i\rangle a^{\dagger}_{m_1,i}a_{m_2,i}, \quad (11)$$

where $|m,i\rangle$ is a ket-vector representation of $\phi_{m,i}(\vec{r})$. The perturbation due to a time-dependent, spatially uniform electric field (e.g., microwaves) in terms of $\vec{u}_{\text{c.m.}}$ is $-eN\vec{E}_0\cdot\vec{u}_{\text{c.m.}}$, where N is the total number of electrons. A quantity whose response to this perturbation is convenient to study is the center of mass displacement itself, so that the response function we will actually focus on is

$$\chi^{\alpha\beta}_{\text{c.m.}}(\tau) = -\langle T_\tau u^{\alpha}_{\text{c.m.}}(\tau)u^{\beta}_{\text{c.m.}}(0)\rangle, \quad (12)$$

where $\alpha,\beta = x,y$.

The conductivity and hence power absorption may be written in terms of this quantity as follows. The time Fourier transform of the spatially averaged current density in response to an applied external field $\text{Re}\,\vec{E}_0 e^{i\omega t}$ is $\langle \vec{j}(\omega)\rangle = ie\rho_0\omega\vec{u}_{\text{c.m.}}(\omega)$, with ρ_0 the sheet density of the electrons. In linear response theory, this takes the form (at zero temperature) $\langle \vec{j}(\omega)\rangle = -ie^2\rho_0\omega N\Sigma_\beta\chi^{\alpha\beta}_{\text{c.m.}}(\omega + i\delta)E^{\beta}_0$, where in the usual way[31] we have Fourier transformed the response function with respect to imaginary time, and made the replacement $i\omega_n \rightarrow \omega + i\delta$ to take the zero-temperature limit. The dot product of this quantity with the total electric field is proportional to the power absorbed. A minor complication is that one must include the screening field generated by the displacements of the electrons. Since we are interested in the bulk current through the system, we assume that the induced electric field may be replaced by its spatial average.[33] Using a dipole approximation for the electric field generated by the motion of the electrons, it is easily shown that $\vec{E}_{\text{ind}}(t) = \frac{e}{2}\alpha\vec{u}_{\text{c.m.}}(t)$, with $\alpha = \Sigma_{i\neq 0}1/R_i^3$. Using $\vec{E}_{\text{tot}} = \vec{E}_0 + \vec{E}_{\text{ind}}$, one finds for the power absorption $\langle \vec{j}(\omega)\rangle\cdot\vec{E}_{\text{tot}} \propto \Sigma_{\alpha,\beta}E^{\alpha}_{\text{tot}}\sigma_{\alpha\beta}(\omega)E^{\beta}_{\text{tot}}$, with the conductivity matrix given by

$$\sigma(\omega) = -ie^2\rho_0\omega N\chi_{\text{c.m.}}(\omega + i\delta)[\mathbf{1} - 2\alpha N\chi_{\text{c.m.}}(\omega + i\delta)]^{-1},$$

where here we are regarding σ and $\chi_{\text{c.m.}}$ as 2×2 matrices. As has been pointed out before,[34] the induced electric field shifts the frequency of the peaks in $\boldsymbol{\sigma}(\omega)$ from where they

are found in $\boldsymbol{\chi}_{\text{c.m.}}(\omega+i\delta)$. However, since the width of the peak we will find in $\boldsymbol{\chi}_{\text{c.m.}}$ is remarkably small, this shift may be neglected for our purposes. Thus in this study we will focus on $\boldsymbol{\chi}_{\text{c.m.}}$ and its frequency dependence.

To compute the center of mass response, we define an intermediate response function

$$\chi^{\alpha}_{m_1m_2}(i;\tau)\equiv\sum_j\sum_{m_3m_4}\langle m_3,j|r^{\alpha}-R^{\alpha}_j|m_4,j\rangle\chi_{m_1m_2m_3m_4}(ij;\tau)$$

in terms of which

$$\chi^{\alpha\beta}_{\text{c.m.}}(\omega)=\frac{1}{N^2}\sum_i\sum_{m_1m_2}\langle m_1,i|r^{\alpha}-R^{\alpha}_i|m_2,i\rangle\chi^{\beta}_{m_1m_2}(i;\omega).$$

Combining the definition of $\chi^{\beta}_{m_1m_2}(i;\tau)$ with Eq. (10), one derives the equation of motion

$$\begin{aligned}i\omega_n\chi^{\beta}_{m_1m_2}(i;i\omega_n)=&\sum_m[\langle\rho_{mm_2}(i)\rangle\langle m|r^{\beta}|m_1\rangle-\langle\rho_{m_1m}(i)\rangle\langle m_2|r^{\beta}|m\rangle]+[\varepsilon_i(m_1)-\varepsilon_i(m_2)]\chi^{\beta}_{m_1m_2}(i;i\omega_n)\\&+\sum_{n_1n_2n_3n_4}\sum_l U'^{il}_{n_1n_2n_3n_4}\{[\chi^{\beta}_{n_1m_2}(i;i\omega_n)\delta_{n_2m_1}-\chi^{\beta}_{m_1n_2}(i;i\omega_n)\delta_{n_1m_2}]\langle\rho_{n_3n_4}(l)\rangle\\&+[\langle\rho_{n_1m_2}(i)\rangle\delta_{n_2m_1}-\langle\rho_{m_1n_2}(i)\rangle\delta_{n_1m_2}]\chi^{\beta}_{n_3n_4}(l;i\omega_n)\}.\end{aligned}\tag{13}$$

Note that the matrix elements $\langle m|r^{\beta}|m_1\rangle$ are the same as those appearing in Eq. (11), evaluated for $\vec{R}_i=0$.

Equation (13) may be solved if one knows the ground state densities $\langle\rho_{m_1m_2}(i)\rangle$. It is here that our assumption that all the electrons reside fully in the lowest angular momentum orbitals for their sites in the ground state becomes useful: the form of the densities is simply $\langle\rho_{m_1m_2}(i)\rangle=\delta_{m_10}\delta_{m_20}$. Furthermore, as shown in the Appendix, it can be proven that $\Sigma_l U'^{il}_{n_1n_200}\propto\delta_{n_1n_2}$, so that Eq. (13) is considerably simplified, taking the form

$$\begin{aligned}&i\omega_n\chi^{\beta}_{m_1m_2}(i;i\omega_n)\\&\quad=\langle 0|r^{\beta}|m_1\rangle\delta_{m_20}-\langle m_2|r^{\beta}|0\rangle\delta_{m_10}\\&\qquad+[\tilde{\varepsilon}_i(m_1)-\tilde{\varepsilon}_i(m_2)]\chi^{\beta}_{m_1m_2}(i;i\omega_n)\\&\qquad+\sum_{n_3n_4}\sum_l[U'^{il}_{0m_1n_3n_4}\delta_{m_2,0}-U'^{il}_{m_20n_3n_4}\delta_{m_1,0}]\\&\qquad\times\chi^{\beta}_{n_3n_4}(l;i\omega_n),\end{aligned}\tag{14}$$

where $\tilde{\varepsilon}_i(m)=\varepsilon_i(m)+\Sigma_l U'^{il}_{mm00}$. It is also easy to show that $\chi^{\beta}_{m_1m_2}=0$ if either m_1 and m_2 are both zero, or if both are nonzero. This is the equation we actually work with, and it is solved in a way closely analogous to the method developed in Ref. 24. We regard $\chi^{\beta}_{m_1m_2}(l)$ as a vector whose components are labeled by m_1,m_2,l. Equation (14) may be written schematically in the form

$$\begin{aligned}&\sum_{n_1,n_2,l}\{[i\omega_n+\Delta\varepsilon_i(m_1,m_2)]\delta_{(i,m_1,m_2),(l,n_1,n_2)}\\&\qquad+U^D_{(im_1m_2),(ln_1n_2)}\}\chi^{\beta}_{n_1n_2}(l;i\omega_n)\\&\quad\equiv[i\omega_n\delta_{(i,m_1,m_2),(l,n_1,n_2)}-M_{(im_1m_2),(ln_1n_2)}]\\&\qquad\times\chi^{\beta}_{n_1n_2}(l;i\omega_n)\\&\quad=\chi^{\beta\,0}_{m_1m_2}(i;i\omega_n),\end{aligned}$$

where $\Delta\varepsilon_i(m_1,m_2)\equiv\tilde{\varepsilon}_i(m_1)-\tilde{\varepsilon}_i(m_2)$ is the energy required to excite an electron on site i from the m_1 orbital into the m_2 orbital when all the other electrons are static,

$$U^D_{(im_1m_2),(ln_1n_2)}=U'^{il}_{0m_1n_3n_4}\delta_{m_2,0}-U'^{il}_{m_20n_3n_4}\delta_{m_1,0}$$

is the change in this energy difference due to the fact that all the electrons are in fact dynamic, and $\chi^{\beta\,0}_{m_1m_2}(i;i\omega_n)=\langle 0|r^{\beta}|m_1\rangle\delta_{m_20}-\langle m_2|r^{\beta}|0\rangle\delta_{m_10}$ is the response function in the absence of both electron-electron interactions and the disorder potential. The matrix M may be diagonalized numerically; it will have real eigenvalues ω_j (which may be shown to come in pairs of equal magnitudes but opposite signs) and eigenvectors $V^j(m_1m_2l)$. It can be shown that when regarded as a matrix in the indices j and (m_1m_2l), V has an inverse V^{-1}. Denoting ω_j as the diagonal matrix of eigenvalues of M, the solution to Eq. (14) may be written schematically as

$$\vec{\chi}^{\beta}(i\omega_n)=\vec{\chi}^{0\,\beta}(i\omega_n)V[i\omega_n\mathbf{1}-\omega_j]^{-1}V^{-1}.$$

From this form, it may be seen that the poles of χ, and hence the energies of collective modes of the system, are given by the set of eigenvalues ω_j.

As a first example, as well as a check on whether this method works, we consider the situation of a WC in an undisordered environment. One only needs then to set $\varepsilon_i(m)=0$ for all i, m in Eq. (14), and proceed as described above. A histogram of the collective mode energies, which represents the density of states for the system, is shown in Fig. 3. In this calculation, the number of electrons was $N=225$, the filling factor was set to $\nu=0.2$, and five states per site were retained. As may be seen, a broad peak near the origin is accompanied by three larger, well-separated peaks at higher energy. The number of such sharp peaks appearing in the

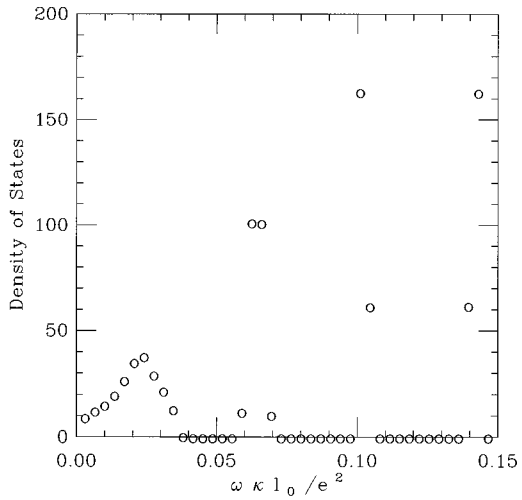

FIG. 3. Collective mode density of states for an unpinned WC as calculated using the quantum harmonic approximation. $N=225$, $\nu=0.2$, and five states per site are retained in the calculation. The result illustrates that including higher-order angular momentum states introduces collective modes at high energy, which may be interpreted as an analog of Frenkel excitons (see text). Such collective modes have little effect on the low-energy dynamics of the system, so that one may drop the high angular momentum states without introducing serious errors in the pinning response of the system.

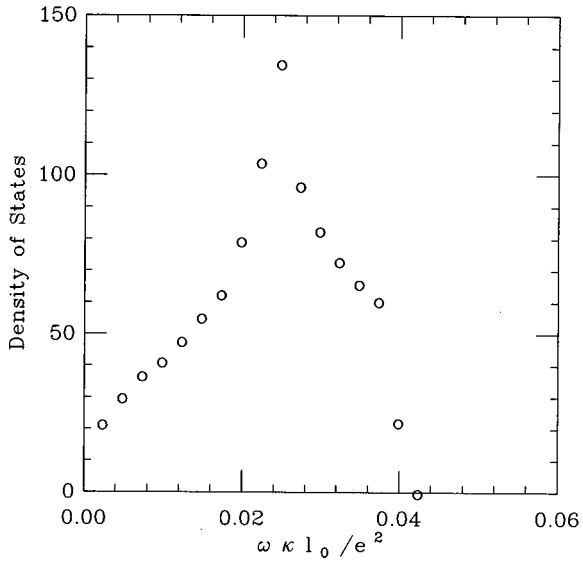

FIG. 4. Collective mode density of states for an unpinned WC as calculated using the quantum harmonic approximation (QHA). $N=1024$, $\nu=0.2$, and two states per site are retained in the calculation. This has a form consistent with the phonon density of states for a classical, unpinned WC in a strong magnetic field, and demonstrates that the QHA produces sensible results for the test case of a WC in the absence of disorder.

density of states we find in general to be equal to the number of orbitals per site above the ground state retained in the calculation.

The meaning of the sharp peaks may be interpreted if one notes that their positions are very close to the values of $\Delta\varepsilon_i(m,0)$ used in the equations of motion. This means that the collective modes are only very weakly affected by U_D, so that one may understand the modes as local excitations in which an electron is excited to a high angular momentum. Thus, these peaks may properly be understood as an analog of Frenkel excitons in tight-binding models of electron systems. Interestingly, these peaks have been previously noted in an approach that does *not* use a harmonic approximation.[24] However, in that approach, the nature of these excitations was unclear; the introduction of the harmonic approximation allows us to understand why there is structure in the density of states at these energies. A careful comparison of the peak positions for $\nu=0.25$ found in Ref. 24 (see Figs. 2 and 3 of that work) with results from the method described here shows that the energies of these peaks are nearly identical for the lowest-energy peaks.

Figure 4 illustrates the density of states for a calculation with $N=529$, $\nu=0.2$, and just two states per site retained. As may be seen, the density of states is precisely what one expects for a phonon density of states in a magnetic field: the leading edge of the phonon density of states rises sharply, consistent with the $D(\omega)\propto\omega^{1/3}$ expected for the low-frequency behavior of the density of states that results from the $\omega(k)\propto k^{3/2}$ dispersion of the WC in a magnetic field.[35] The peak contains a strong cusp structure consistent with a van Hove singularity, and the width of the peak is found to decrease with increasing magnetic field, consistent with the $1/B$ dropoff expected for the phonon bandwidth.[35]

The quantitative agreement of these results with previous calculations gives a strong indication that the QHA works, and we learn from the above calculations that all the low-energy modes (i.e., phonons) of the WC can be captured by retaining just two states per site. This considerable simplification allows one to treat fairly large numbers of electrons for the pinned WC; our largest calculations contain $N=1024$ electrons. From this point onward we will adopt the two-state approximation, and denote the energy difference between the two states on a site as $\Delta\varepsilon_i(m=1,0)$ as $\Delta\varepsilon_i$.

Having established that the QHA gives sensible results for cases where the correct answer is known, we can now use it to investigate the case of the pinned WC. We defer detailed discussions of the results to Sec. V; however, they can be summarized extremely briefly. Essentially all of our center of mass response functions are dominated by a single collective mode, the lowest excited state arising for any given disorder realization (e.g., Fig. 1). For the weak disorder models [i.e., $\Delta\varepsilon_i \ll \omega_B$, where ω_B is the bandwidth of the phonon density of states (Fig. 4)], the position of the pinning frequency turns out to be extremely close to v_0, the average pinning energy per site. We find this form of the center of mass response for all our disorder models and system sizes studied, and there is no noticeable trend for the strength of this one mode to decrease with increasing system size within the sizes one may study using this model. One is led to conclude that the electromagnetic response of the WC in a strong magnetic field at zero temperature is extremely sharp, consistent with experiment but not with previous theoretical expectations. As explained in the Introduction, this turns out to be a consequence of the long-range nature of the Coulomb interaction. To see precisely how this result arises, as well as to assess whether it will survive in the thermodynamic limit, we need to develop an approach from which one may learn what happens to this mode for very large systems. This is the subject of the next section.

III. PSEUDOSPIN REPRESENTATION

The results of the QHA indicate that generically there is a sharp resonance in the low-frequency response of the magnetically induced WC for the finite size systems one is able to handle with that method. While there is no indication within those calculations that the resonance either broadens or weakens with increasing system size, one cannot rule out based upon them the possibility that a broadening does develop at very large system sizes. Thus one would like to develop models that are analytically tractable wherein the thermodynamic limit may be taken.

A. Quantum Spin Model

In this subsection we will develop a mapping of the electron system onto an effective spin lattice system, and obtain couplings between these spins using an expansion in l_0/a_0, with a_0 the nearest neighbor distance. One important advantage of this formulation is that the resulting couplings are far more tractable than the matrix elements found in the QHA, allowing us to make considerable progress analytically. The spin waves of the model are the analog of the phonons for the WC, and it will be shown that the resulting dispersion of these spin waves is identical to the classical phonon spectrum of the WC, demonstrating that the mapping produces sensible results.

We begin with the observation from the QHA analysis that essentially all the low-energy excitations of the magnetically induced WC may be obtained in a model that retains only two states per lattice site. This motivates an approach in which one may wish to consider the on-site degrees of freedom of each electron as an effective pseudospin, with the $m=0$ angular momentum state representing a ''spin up'' state, and the $m=1$ a ''spin down'' state. (Note that we will assume the real spins of the electrons are polarized by the magnetic field and do not represent a low-energy degree of freedom for the system.) The system is then mapped onto a quantum magnet, whose interactions we will see are of a magnetic dipole form, and whose spin waves will have the same dispersion relation as the phonon spectrum of the underlying classical electron degrees of freedom. Formally, the mapping is given by

$$\begin{aligned} a_{0j}^{\dagger}a_{0j}-a_{1j}^{\dagger}a_{1j} &\rightarrow 2S_j^z, \\ a_{0j}^{\dagger}a_{1j} &\rightarrow S_j^{+}, \\ a_{1j}^{\dagger}a_{0j} &\rightarrow S_j^{-}. \end{aligned} \tag{15}$$

To write an effective Hamiltonian for these pseudospin degrees of freedom, it is convenient to employ a multipole expansion of the electron density, which becomes quantitatively accurate in the limit $l_0/a_0 \ll 1$ (i.e., $\nu \ll 1$), where a_0 is the nearest neighbor distance. Neglecting exchange effects, the interaction energy is formally

$$U=\frac{e^2}{2}\sum_{i\neq j}\int d^2r_1 d^2r_2 \frac{\rho(\vec{r}_1+\vec{R}_i)\rho(\vec{r}_2+\vec{R}_j)}{|\vec{R}_i+\vec{r}_1-\vec{R}_j-\vec{r}_2|}. \tag{16}$$

Writing $\rho(\vec{r}+\vec{R}_i)\equiv\rho_i(\vec{r})$, the densities may be written in terms of the pseudospin operators,

$$\begin{aligned} \rho_i(\vec{r}) = &|\phi_0^2(\vec{r})|^2[\tfrac{1}{2}+S_i^z]+|\phi_1^2(\vec{r})|^2[\tfrac{1}{2}-S_i^z] \\ &+\phi_0^*(\vec{r})\phi_1(\vec{r})S_i^{-}+\phi_1^*(\vec{r})\phi_0(\vec{r})S_i^{+} \end{aligned} \tag{17}$$

where $\phi_{0(1)}$ are the $m=0(1)$ orbitals localized around the site of interest [Eq. (3)], and we have suppressed the explicit site labels $i(j)$. Substituting Eq. (17) into Eq. (16), expanding the integrand to second order in $r_{1(2)}/R_{ij}$ where $R_{ij}\equiv|\vec{R}_i-\vec{R}_j|$, and performing the integrations, one arrives at the formula $U=\frac{1}{2}\Sigma_{i\neq j}U_{ij}$, with

$$\begin{aligned} U_{ij}=&\frac{e^2}{R_{ij}}+\frac{3e^2l_0^2}{2R_{ij}^3}-\frac{e^2l_0^2}{2R_{ij}^3}[S_i^z+S_j^z] \\ &+\frac{2e^2l_0^2}{R_{ij}^3}[S_i^{\parallel}\cdot S_j^{\parallel}-3(S_i^{\parallel}\cdot\vec{R}_{ij})(S_j^{\parallel}\cdot\vec{R}_{ij})/R_{ij}^2], \end{aligned}$$

where $S_{i(j)}^{\parallel}\equiv(S_{i(j)}^x,S_{i(j)}^y,0)$. Note that the effective interaction between spins in U_{ij} is of an XY dipole form, which is not surprising given the fact that a small r expansion for the electron-electron interaction leads to an electric dipole interaction. The third term in U_{ij} takes the form of an effective magnetic field that tends to orient the spins in the $+\hat{z}$ direction; this reflects the fact that the ϕ_0 state is the ground state of an electron in a given site if all the other electrons are fixed in their ϕ_0 states. The Hamiltonian for the effective spin system thus may be written in the form

$$H=\sum_i h_i S_i^z+\sum_{\alpha,\beta}\sum_{i\neq j}J_{ij}^{\alpha,\beta}S_i^{\alpha}S_j^{\beta}, \tag{18}$$

where $\alpha,\beta=x,y$, $J_{ij}^{\alpha,\beta}=(e^2l_0^2/R_{ij}^3)[\delta_{\alpha,\beta}-3R_{ij}^{\alpha}R_{ij}^{\beta}/R_{ij}^2]$, and $h_i=-\Sigma_{j(\neq i)}(e^2l_0^2/2R_{ij}^3)+\varepsilon_i(m=0)-\varepsilon_i(m=1)$ is an effective magnetic field, which may be nonuniform due to the pinning potential. Note that we have dropped an irrelevant constant from the Hamiltonian.

The low-energy collective modes of this model are spin waves, and in the absence of a pinning potential their dispersion relation should be identical to that of the phonon modes of the underlying WC from which the pseudospin model was derived. We thus begin our analysis by considering the case $\varepsilon_i(m)=0$. To derive the spin-wave spectrum, we rewrite the spin operators in terms of bosonic degrees of freedom[36] with the approximate mapping

$$\begin{aligned} S_i^z &\rightarrow \frac{1}{2}-b_i^{\dagger}b_i, \\ S_i^{+} &\rightarrow b_i, \\ S_i^{-} &\rightarrow b_i^{\dagger}. \end{aligned} \tag{19}$$

This mapping is an approximate form of the Holstein-Primakoff transformation,[37] expanded for the situation $\langle b_i^{\dagger}b_i\rangle \ll 1/2$, where $\langle\ \rangle$ is an expectation value for any of the low-energy states that are of interest in the zero temperature response function. A simple way to see that $\langle b_i^{\dagger}b_i\rangle$ is small is to write it directly in terms of the underlying electron creation and annihilation operators: $b_i^{\dagger}=a_{1i}^{\dagger}a_{0i}, b_i=a_{0i}^{\dagger}a_{1i}$.

One then finds $[b_i, b_i^\dagger] = a_{0i}^\dagger a_{0i} - a_{1i}^\dagger a_{1i}$. If the mapping were exact, this commutator would be unity. However, to the extent that the ground state is well approximated by electrons in Gaussian orbitals, $\langle a_{0i}^\dagger a_{0i}\rangle = 1$ and $\langle a_{1i}^\dagger a_{1i}\rangle = 0$ in the ground state. Furthermore, the lowest excited states — the spin waves in the bosonic language — are described in terms of the electronic degrees of freedom by a single particle excited out of the $m=0$ state into the $m=1$ state, averaged with an appropriate phase factor over all the sites. Thus the expectation value of $[b_i, b_i^\dagger]$ for the low-lying states is the same as that of the ground state, up to corrections that vanish in the thermodynamic limit. It should be noted that when quantum (or, at finite temperature, thermal) fluctuations are important, then one must work with the exact mapping between spin and boson operators,[37] and higher-order terms in $b_i^\dagger b_i$ should be retained, introducing spin-wave interactions. Such terms are the analog of anharmonic terms in the Hamiltonian for the underlying WC degrees of freedom, and we expect them to be very small at zero temperature for large magnetic fields (small ν), where placing the electron in Gaussian orbitals at specified locations that minimize the potential energy is thought to be an excellent approximation for the ground state.[20] From this point onward we will ignore spin-wave interactions, and our goal will be to understand why disorder does not broaden the electromagnetic response associated with the quadratic Hamiltonian below.

In terms of the bosonic operators, the Hamiltonian we thus will consider takes the form

$$H = \sum_i U_i b_i^\dagger b_i + \sum_{i\neq j} \frac{e^2 l_0^2}{R_{ij}^3} \times \left\{ -\frac{1}{4}(b_i^\dagger b_j + b_i b_j^\dagger) - \frac{3}{4}[(n_{ij}^*)^2 b_i^\dagger b_j^\dagger + (n_{ij})^2 b_i b_j] \right\}. \tag{20}$$

Here, $U_i = -h_i$, and $n_{ij} = (R_{ij}^x - iR_{ij}^y)/R_{ij}$ is a complex representation of the vector direction separating sites R_i and R_j. In the absence of pinning $[\varepsilon_i(m) = 0]$, H is diagonalized in two steps. First, a canonical transformation from real to momentum space separates out the independent modes:

$$H = \sum_{\vec{k}} F(\vec{k}) b_{\vec{k}}^\dagger b_{\vec{k}} - \sum_{\vec{k}} [G(\vec{k}) b_{\vec{k}} b_{-\vec{k}} + G^*(\vec{k}) b_{-\vec{k}}^\dagger b_{\vec{k}}^\dagger],$$

where $b_{\vec{k}} = (1/N^{1/2}) \sum_i e^{i\vec{k}\cdot\vec{R}_i} b_i$, $F(\vec{k}) = \frac{1}{2}\sum_j (e^2 l_0^2/R_j^3)(1 - e^{-i\vec{k}\cdot\vec{R}_j})$, and $G(\vec{k}) = \frac{3}{4}\sum_{\vec{R}_j\neq 0} (e^2 l_0^2/R_j^3)(n_{\vec{R}_j})^2 e^{i\vec{k}\cdot\vec{R}_j}$. The diagonalization of the Hamiltonian is then completed with a Bogoliubov transformation of the form $\gamma_{\vec{k}} = u_{\vec{k}} b_{\vec{k}} + v_{\vec{k}} b_{-\vec{k}}^\dagger$, with $|u_{\vec{k}}|^2 - |v_{\vec{k}}|^2 = 1$ guaranteeing that $[\gamma_{\vec{k}}, \gamma_{\vec{k}}^\dagger] = 1$. The boson Hamiltonian then may be written as $H = \sum_{\vec{k}} E_{\vec{k}} \gamma_{\vec{k}}^\dagger \gamma_{\vec{k}}$ if one chooses

$$u_{\vec{k}} = \cosh\theta_{\vec{k}} e^{i\phi_{\vec{k}}/2},$$
$$v_{\vec{k}} = \sinh\theta_{\vec{k}} e^{-i\phi_{\vec{k}}/2}, \tag{21}$$
$$E_{\vec{k}} = \sqrt{F(\vec{k})^2 - 4|G(\vec{k})|^2},$$

with $G(\vec{k}) = e^{i\phi_{\vec{k}}}|G(\vec{k})|$, and $\tanh 2\theta_{\vec{k}} = -2|G(\vec{k})|/F(\vec{k})$.

$E_{\vec{k}}$ thus represents the spin-wave dispersion for this model, and we need to confirm that it has the same form as the underlying electron degrees of freedom. For the WC in two dimensions in the absence of a magnetic field, the phonon dispersion is found by solving the eigenvalue equation[38]

$$\sum_\beta C_{\alpha\beta}(\vec{k}) e_\beta = \omega^2(\vec{k}) e_\beta, \tag{22}$$

where

$$C_{\alpha\beta}(\vec{k}) = -\frac{e^2}{m^*}\left\{ \sum_j \left(\frac{3R_j^\alpha R_j^\beta}{R_j^5} - \frac{\delta_{\alpha,\beta}}{R_j^3} \right)(e^{-i\vec{k}\cdot\vec{R}_j} - 1) \right\} \tag{23}$$

and m^* is the effective mass of the electrons. For every value of $\vec{k}$, Eq. (22) has two eigenvalues, corresponding to a longitudinal mode $\omega_l(\vec{k})$ and a transverse mode $\omega_t(\vec{k})$. In the presence of a magnetic field, the equations of motion for the electrons mix these two modes. One then obtains two different normal modes, one dispersing from the cyclotron frequency $\omega_c = eB/m^*c$, and the other having the form in the strong field limit[35] $\omega(\vec{k}) = \omega_l(\vec{k})\omega_t(\vec{k})/\omega_c$. By solving Eq. (22) and using Eq. (23), one may show with some algebra that $\omega_l(\vec{k})\omega_t(\vec{k})/\omega_c \equiv E_{\vec{k}}$. Thus the spin waves of our pseudospin model faithfully reproduce the exact phonon spectrum for the WC in a strong magnetic field, and we see that our model quantitatively captures the low-energy dynamics of the WC.

B. Uniformly pinned Wigner crystal

In this subsection we will analyze the response function of a WC in which each site has precisely the same pinning potential. We will find that the power absorption from a spatially uniform, time-varying electric field is sharp as a function of frequency. This result is hardly surprising as there is no disorder in this model. However, it will serve as the basis for the perturbative treatment in the next subsection, and so is useful to analyze in some detail.

To introduce uniform pinning in the model, one only needs to set $h_i = -\Sigma_{\vec{R}\neq 0}(e^2 l_0^2/2R^3) - v_0$ for all the sites i in Eq. (18). The representation of the spin wave Hamiltonian in terms of phonon degrees of freedom, and its diagonalization, are formally identical to the steps used in the preceding subsection, provided one makes the replacement

$$F(\vec{k}) \to F(\vec{k}) + v_0 \equiv F_p(\vec{k}).$$

The resulting (pseudo)spin wave for this model is thus

$$E_k^p = \sqrt{F_p(\vec{k})^2 - 4|G(\vec{k})|^2}. \tag{24}$$

In the limit $k \to 0$, $E_{\vec{k}}^p \to v_0$. Thus for collective modes in which all the electrons move together, only the center of mass degree of freedom is relevant: electron-electron interactions may be ignored, and one obtains the single electron excitation frequency.[21] The long wavelength dispersion of Eq. (24) may be obtained by evaluating $F(\vec{k})$ and $G(\vec{k})$ using an Ewald sum technique.[38] One finds

$$F(\vec{k}) \approx 2\pi e^2 l_0^2 \rho_0 k + O(k^2), \tag{25}$$

$$G(\vec{k}) \approx \pi e^2 l_0^2 \rho_0 (k_x + i k_y)^2 / k + O(k^2), \tag{26}$$

so that

$$E_{\vec{k}}^p \approx v_0 + 2\pi e^2 l_0^2 \rho_0 k + O(k^2). \tag{27}$$

The linear dispersion of the pinned collective mode spectrum is purely a result of the long-range nature of the Coulomb interaction. For a short-range interaction, the collective mode disperses instead as k^2 from v_0. The linear dispersion, and hence the long-range nature of the Coulomb interaction, turns out to play a crucial role in allowing the sharp response of the uniformly pinned system to survive the introduction of disorder. This will be discussed more carefully in the next subsection.

Because one may exactly diagonalize the Hamiltonian in this model, it is convenient to compute the power absorption using Fermi's golden rule. For an electric field of the form $\vec{E}(t) = \mathrm{Re}\, E_0(\hat{x} + i\hat{y}) e^{i\omega t}$, one obtains for zero temperature

$$P(\omega) = N\pi e^2 E_0^2 l_0^2 \sum_n E_n^p |\langle n | \gamma_{\vec{k}=0}^\dagger | 0 \rangle|^2 \delta(\omega - E_n^p), \tag{28}$$

where $|0\rangle$ is the ground state of the system (no spin waves), and $|n\rangle$ represents the set of single pseudospin wave excitations (which in the present case may be labeled by $\vec{k}$ rather than n). For the uniformly pinned system, the matrix element entering Eq. (28) is nonvanishing only for $E_{\vec{k}}^p = v_0$, so that one obtains a δ function response at $\omega = v_0$, as expected.

Equation (28) is a good starting point for a perturbative treatment of disorder effects. In particular, the weight arising from the matrix element $\langle n | \gamma_{\vec{k}=0} | 0 \rangle$ must remain proportional to the system size in the thermodynamic limit for one particular mode n if the system is to retain the sharp response observed in Sec. II for an arbitrarily large system. In the next subsection, we show that, at least for weak disorder, this is indeed the case.

C. Weak disorder: Perturbative treatment

In this subsection, we will formulate a perturbation theory for Eq. (28), in terms of deviations of the pinning potential from uniformity. The point of this analysis is to understand how the sharpness of the response might survive the introduction of disorder. Towards this end, we will focus on the height of the δ-function response found in the preceding subsection, and develop an expression to the lowest nontrivial order in perturbation theory to see how much it is decreased by disorder. The resulting expression, when disorder averaged, will turn out to have a formal, logarithmic divergence, which we interpret to mean that there is no true δ-function response in the thermodynamic limit. However, the divergence is in fact cut off by the system size, and we will see that even a conservative estimate of the integral for real system sizes indicates that it is in fact small, so that the perturbation theory is valid. The integral allows us to define a length L_c that is the characteristic size scale for electrons moving together in phase in the lowest collective mode, and we will see that L_c is extremely large compared to real sample dimensions.

The quantity we will use for our perturbing parameter is the deviation of the pinning potential from perfect uniformity, ΔU_i, which is formally defined by the equation $h_i = -\Sigma_{\vec{R}\neq 0}(e^2 l_0^2 / 2R^3) - v_0 - \Delta U_i$. Note from its definition that $\Sigma_i \Delta U_i = 0$, a property we will use below. The power absorption [Eq. (28)] may be written via standard many-body manipulations[31] in terms of a Green's function, in the form

$$P(\omega) = -e^2 l_0^2 E_0^2 \omega \mathrm{Im} \left\{ \sum_{\mu\nu} \sum_{ij} d_\mu^0(i) d_\nu^0(j)^* \times G_{\mu\nu}(ij; \omega + i\delta) \right\}. \tag{29}$$

The Green function matrix entering above is given in imaginary time by

$$G_{\mu,\nu}(ij;\tau) = -\langle T_\tau b_i^{(\mu)}(\tau) b_j^{(\nu)\dagger}(0) \rangle, \tag{30}$$

with $\mu, \nu = 1,2$, $b_i^{(1)} = b_i$, and $b_i^{(2)} = b_i^\dagger$. The c-numbers $d_\mu^0(i)$ entering Eq. (29) are those that diagonalize the pseudospin-wave Hamiltonian Eq. (20) for the $\vec{k}=0$ mode in the uniformly pinned case [i.e., $d_1^0(i) \equiv v_{\vec{k}=0} = 0, d_2^0(i) \equiv u_{\vec{k}=0} = 1$, with u, v given by Eq. (21)]. Using the method described in Sec. II and Eq. (20), the equation of motion for the Green function in imaginary time is found to be

$$\begin{aligned} -i\omega_n \begin{pmatrix} G_{11}(ij;i\omega_n) \\ G_{21}(ij;i\omega_n) \end{pmatrix} &= -\delta_{ij} \begin{pmatrix} 1 \\ 0 \end{pmatrix} + \Delta U_i \begin{bmatrix} -1 & 0 \\ 0 & 1 \end{bmatrix} \begin{pmatrix} G_{11}(ij;i\omega_n) \\ G_{21}(ij;i\omega_n) \end{pmatrix} \\ &\quad + \sum_k \begin{bmatrix} -F_p(\vec{R}_i - \vec{R}_k) & -2G^*(\vec{R}_i - \vec{R}_k) \\ 2G(\vec{R}_i - \vec{R}_k) & F_p(\vec{R}_i - \vec{R}_k) \end{bmatrix} \\ &\quad \times \begin{pmatrix} G_{11}(kj;i\omega_n) \\ G_{21}(kj;i\omega_n) \end{pmatrix}, \end{aligned} \tag{31}$$

where

$$F_p(\vec{R}) = \frac{e^2 l_0^2}{2} \sum_{\vec{R}'\neq 0} \frac{1}{R'^3} [\delta_{\vec{R},0} - \delta_{\vec{R},\vec{R}'}](1 - \delta_{\vec{R},0}) + v_0 \delta_{\vec{R},0},$$

$$G(\vec{R}) = \frac{3e^2 l_0^2}{4R^3} n_{\vec{R}}^2 (1 - \delta_{\vec{R},0}). \tag{32}$$

Note the the quantities in Eq. (32) are just the discrete Fourier transforms of the quantities $F_p(\vec{k})$ and $G(\vec{k})$ defined in the preceding subsection. The matrix elements G_{12} and G_{22} may be found by using $G_{12}(ij;i\omega_n) = G_{21}^*(ij;-i\omega_n)$ and $G_{22}(ij;i\omega_n) = G_{11}^*(ij;-i\omega_n)$.

Equation (31) may be solved in a manner closely analogous to that of Sec. II: one needs to solve the eigenvalue equation

$$\sum_k \begin{bmatrix} -\Delta U_i \delta_{ik} - F_p(\vec{R}_i - \vec{R}_k) & -2G^*(\vec{R}_i - \vec{R}_k) \\ 2G(\vec{R}_i - \vec{R}_k) & \Delta U_i \delta_{ik} + F_p(\vec{R}_i - \vec{R}_k) \end{bmatrix} \times \begin{pmatrix} d_1^{(j)}(k) \\ d_2^{(j)}(k) \end{pmatrix} = \omega_j \begin{pmatrix} d_1^{(j)}(i) \\ d_2^{(j)}(i) \end{pmatrix}, \tag{33}$$

and then the solution may be expressed in terms of the eigenvalues and eigenvectors. It is not difficult to prove several properties of the solutions to Eq. (33) based on the symmetry of the matrix.[39] In particular, one may easily show that the eigenvalues come in pairs of equal magnitude and opposite sign, $\pm\omega_j$. The eigenvector of the solution with negative ω_j may be found from the solution with positive ω_j with the transformation

$$d_1^{(-)}(k) = d_2^{(+)*}(k), \quad d_2^{(-)}(k) = d_1^{(+)*}(k).$$

Because the matrix being diagonalized is not Hermitian, these two eigenvectors are not in general orthogonal to one another. If one imposes the normalization condition $\Sigma_k[|d_2^{(j)}(k)|^2 - |d_1^{(j)}(k)|^2] = 1$ for positive eigenvalues ($\omega_j > 0$) and insists that the eigenvectors associated with each pair of eigenvalues of the same magnitude obey the above relation, the inverse of the eigenvector matrix may be explicitly constructed. Writing this as $e_\mu^{(j)}(k)$ so that $\Sigma_{\mu,k} e_\mu^{(j)}(k) d_\mu^{(j')}(k) = \delta_{j,j'}$, we find

$$e_1^{(j)}(k) = -d_1^{(j)*}(k), \quad e_2^{(j)}(k) = d_2^{(j)*}(k)$$

for $\omega_j > 0$, and

$$e_1^{(j)}(k) = d_1^{(j)*}(k), \quad e_2^{(j)}(k) = -d_2^{(j)*}(k)$$

for $\omega_j < 0$. With this explicit expression for the eigenvector matrix inverse, it is possible to write the solution to Eq. (31) as

$$G_{\mu\nu}(ik; i\omega_n) = \sum_j \frac{d_\mu^{(j)}(i) e_\nu^{(j)}(k)}{i\omega_n + \omega_j}$$

for $(\mu\nu) = (11)$ and (21). For $(\mu\nu) = (22)$ and (12), the expression is the same as above, except one needs to take the complex conjugate of the numerator. Combining this with Eq. (29), and noting that $d_1^0(i) = 0$ so that $\Sigma_{ik}\Sigma_{\mu\nu} d_\mu^0(i) e_\mu^{(j)}(i)^* d_\nu^{(j)}(k)^* d_\nu^0(k)$ is purely real, it follows that

$$P(\omega) = e^2 I_0^2 E_0^2 \omega \pi \sum_j \left[\sum_i d_2^0(i) e_2^{(j)}(i)^* \right] \times \left[\sum_k d_2^0(k)^* d_2^{(j)}(k)^* \right] \delta(\omega - \omega_j) \tag{34}$$

for $\omega > 0$.

For a finite size system, Eq. (34) describes absorption by the system into a discrete set of states, with a weight that may be interpreted as the square overlap of the mode being excited with eigenvector of the $\vec{k} = 0$ mode for the uniformly pinned case. In most situations, one expects as the thermodynamic limit is approached that the weight associated with each mode vanishes with increasing system size, while the density of modes increases, to generate an absorption curve that is a continuous function of frequency. What we have found in Sec. II seems to imply that the lowest mode in the spectrum of the disordered system retains a much larger overlap than all the other modes, even for large systems. To understand how this arises, we need to compute the overlap sum $[\Sigma_i d_2^0(i) e_2^{(j)}(i)^*][\Sigma_k d_2^0(k)^* d_2^{(j)}(k)^*]$ in Eq. (34) for the lowest-energy mode, and see how it scales with increasing system size. Although an exact calculation of this quantity is not possible for an arbitrary disorder strength and arbitrarily large system, we can at least estimate it for weak disorder to see if and when a finite overlap survives in the thermodynamic limit.

Towards this end, we compute the eigenvectors of the matrix in Eq. (33) to second order in ΔU_i. The method by which this is done is identical to standard nondegenerate perturbation theory in quantum mechanics.[40] Denoting $(d_1^{(j)}(\vec{R}_1), d_1^{(j)}(\vec{R}_2), \ldots, d_2^{(j)}(\vec{R}_1), d_2^{(j)}(\vec{R}_2), \ldots) \equiv \mathbf{V}^{(j)}$, we may write the result of the calculation as

$$\mathbf{V}^{(j)} = [1 - D(j)]^{1/2} \mathbf{V}_0^{(j)} + \sum_{k(\neq i)} \mathbf{V}_0^{(k)} \left[\frac{\langle k|\Delta U|j\rangle}{E_j^{(0)} - E_k^{(0)}} + O(\Delta U_i^2) \right], \tag{35}$$

where $\mathbf{V}_0^{(j)}, E_j^0$ are the eigenvectors and eigenvalues in the absence of the perturbation. The matrix element is given by

$$\langle k|\Delta U|j\rangle = \mathbf{W}_0^{(k)T} \begin{pmatrix} -\Delta U & 0 \\ 0 & \Delta U \end{pmatrix} \mathbf{V}_0^{(j)},$$

with $\mathbf{W}_0^{(k)T}$ representing a column vector of the form $(e_1^{(j)}(\vec{R}_1), e_1^{(j)}(\vec{R}_2), \ldots, e_2^{(j)}(\vec{R}_1), e_2^{(j)}(\vec{R}_2), \ldots)$, and ΔU in the above matrix is an $N \times N$ diagonal matrix with entries ΔU_i on the diagonal. The relevant quantity for our purpose is the ''depletion'' $D(j)$, which one finds to be

$$D(j) = \sum_{k(\neq j)} \left| \frac{\langle k|\Delta U|j\rangle}{E_j^{(0)} - E_k^{(0)}} \right|^2 + O(\Delta U^3). \tag{36}$$

The zeroth-order eigenvectors and eigenvalues are easily evaluated, as these were already essentially found in the preceding subsection. Thus the eigenvectors without disorder are conveniently labeled by a wave vector $\vec{q}$ and a sign $\pm$ denoting whether the positive or negative eigenvalue for a given wave vector is being referred to. Thus we use the eigenvalues $E_j^0 = \pm E_{\vec{q}} = \pm[F_p(\vec{q})^2 - 4|G(\vec{q})|^2]^{1/2}$, and the corresponding eigenvectors have the form $d_1^{(\vec{q})}(i) = (1/\sqrt{N})\, e^{i\vec{q}\cdot\vec{R}_i} v_{\vec{q}}, d_2^{(\vec{q})}(i) = (1/\sqrt{N})\, e^{i\vec{q}\cdot\vec{R}_i} u_{\vec{q}}$, with

$$u_{\vec{q}} = u_{\vec{q}}^+ = \left[\frac{F_p(\vec{q}) + E_{\vec{q}}}{2E_{\vec{q}}} \right]^{1/2} e^{i\phi_{\vec{q}}/2},$$

$$v_{\vec{q}} = v_{\vec{q}}^+ = -\frac{2|G(\vec{q})|}{\sqrt{2E_{\vec{q}}}} \left[\frac{1}{F_p(\vec{q}) + E_{\vec{q}}} \right]^{1/2} e^{-i\phi_{\vec{q}}/2} \tag{37}$$

for $E_j^0 > 0$, and

$$u_{\vec{q}}=u_{\vec{q}}^{-}=-\frac{2|G(\vec{q})|}{\sqrt{2E_{\vec{q}}}}\left[\frac{1}{F_p(\vec{q})+E_{\vec{q}}}\right]^{1/2}e^{i\phi_{\vec{q}}/2},$$
$$v_{\vec{q}}=v_{\vec{q}}^{-}=\left[\frac{F_p(\vec{q})+E_{\vec{q}}}{2E_{\vec{q}}}\right]^{1/2}e^{-i\phi_{\vec{q}}/2} \tag{38}$$

for $E_j^0<0$. Since the factors d_2^0 appearing in the power absorption [Eq. (34)] are just the non-zero part of the eigenvectors above for $q=0$, it is easy to verify that the weight associated with excitations into the lowest collective mode in power absorption is just $1-D(0)$ [i.e., there will be a contribution to the sum over modes appearing in Eq. (34) proportional to $1-D(0)$.] Provided $D(0)\ll 1$, this will remain a δ-function contribution at zero temperature, even as absorption into the other modes may merge into a broad background. Thus $D(0)$ measures the depletion of the sharp pinning mode response found for the uniformly pinned model. It should be noted that because of our choice of system around which we are doing perturbation theory, there are no corrections to the pinning mode frequency at $O(\Delta U)$; the first nonvanishing correction is of $O(\Delta U^2)$, so that the frequency of the pinning mode remains close to its uniformly pinned value.

Using the forms for the uniformly pinned model in Eq. (36), one finds

$$D(0)=\frac{1}{N}\sum_{\vec{q}\neq 0}\left\{\frac{|u_{\vec{q}}^{+}|^2|\Delta U(\vec{q})|^2}{[v_0-E_{\vec{q}}]^2}+\frac{|u_{\vec{q}}^{-}|^2|\Delta U(\vec{q})|^2}{[v_0+E_{\vec{q}}]^2}\right\}, \tag{39}$$

with $\Delta U(\vec{q})=(1/\sqrt{N})\,\Sigma_i \Delta U_i e^{i\vec{q}\cdot\vec{R}_i}$. The second term in Eq. (39) is always finite and is small provided $|\Delta U(\vec{q})/E_q|^2$ is small. The first may potentially diverge even for small $|\Delta U(\vec{q})|$ because $E_{\vec{q}}\to v_0$ as $\vec{q}\to 0$, so that there is a vanishing energy denominator. However, for a given disorder realization, by our choice of the system around which we are performing perturbation theory, we have $|\Delta U(\vec{q})|\propto q^2$ for small q. The energy denominator, using Eq. (27), behaves as $[v_0-E_{\vec{q}}]^2\approx(2\pi e^2 l_0^2\rho_0 q)^2$, so that the integral remains finite, and can be small if $\Delta U(\vec{q})$ is small enough.

This is the central result of this section, and several comments are in order. First, the result of Eq. (39) is only finite in this analysis because of the long-range nature of the interaction. For short-range interactions, $[v_0-E_{\vec{q}}]^2\propto q^4$, and one ends up with a divergence no matter how small $|\Delta U(\vec{q})|$ might be. Such a divergence indicates that one cannot stop at second order in the perturbation as we have done here, and that some self-consistent treatment is called for.[7,18] Under these circumstances, one expects the resulting response to be broad, as is the case for most pinned CDW's.[6] As mentioned in the Introduction, this is borne out by the QHA of Sec. II, which shows that a broad response is indeed obtained if one uses a screened rather than long-range Coulomb potential (cf. Fig. 2). Secondly, in many calculations where one averages over disorder configurations, the simplest choice of disorder models (white noise) introduces fluctuations at all length scales, so that the disorder average $\overline{|\Delta U(\vec{q})|^2}\equiv\overline{|\Delta U|^2}$ is independent of wave vector. Thus, a disorder average of Eq. (39) would eliminate the zero in the numerator as $\vec{q}\to 0$, and introduce a logarithmically divergent depletion in the thermodynamic limit, signaling a broadened rather than sharp response.

In practice, however, we find that for physically relevant systems the response remains sharp. The reason for this is that the divergence only arises for truly infinite systems. We can define a length scale L_c above which the depletion $D(0)$ is of order 1, so that the δ-function response becomes significantly broadened. To do this, one must solve the equation

$$1=\frac{1}{\rho_0}\int_{q>2\pi/L_c}\frac{d^2q}{(2\pi)^2}\overline{|\Delta U|^2}\left\{\frac{|u_{\vec{q}}^{+}|^2}{[v_0-E_{\vec{q}}]^2}+\frac{|u_{\vec{q}}^{-}|^2}{[v_0+E_{\vec{q}}]^2}\right\}. \tag{40}$$

We can break up this integral into singular and nonsingular parts as $L_c\to\infty$, and so write Eq. (40) in the form

$$1=\frac{1}{2\pi\rho_0}\int_{2\pi/L_c}^{2\pi/\ell}\frac{dq}{q}\frac{\overline{|\Delta U|^2}}{2\pi e^2 l_0^2\rho_0^2}+\eta(\ell),$$

where we have used Eq. (27). In the above equation, ℓ represents a length scale above which the collective mode dispersion for the uniformly pinned system is accurately represented by Eq. (27) ($\ell\approx 10a_0$ would probably be sufficiently large), and $\eta(\ell)$ represents the nonsingular contribution to Eq. (40). One may now solve for L_c, with the result

$$L_c=\ell\exp\left\{\frac{(2\pi\rho_0)^3(el_0)^4}{\overline{|\Delta U|^2}}[1-\eta(\ell)]\right\}$$
$$=\ell\exp\left\{\frac{\nu^3}{|\Delta\tilde{U}|^2}[1-\eta(\ell)]\right\}. \tag{41}$$

In Eq. (41), $|\Delta\tilde{U}|^2$ is the disorder potential strength $\overline{|\Delta U^2|}$ written in units of $e^2/\kappa l_0$. For weak disorder, $\eta(\ell)\ll 1$. We will discuss the interpretation and consequences of Eq. (41) further in Sec. V below; for now, however, we point out that an estimate of L_c for physically relevant parameters shows that it is extremely large, much larger than the physical dimensions of any real sample. This means that in practice, the depletion $D(0)$ will be small for weak disorder, since the sample size cuts off the divergence at length scales much smaller than the one at which broadening becomes significant.

It is interesting to consider what would happen if one were to consider a model in which the displacement of electrons from their lattice sites was included as an effect of the disorder. The essential change is that the electron centers $\vec{R}_i$ appearing in Eq. (31) are no longer on lattice sites. For weak disorder, if one neglects lattice defects such as dislocations and disclinations, the effect of the lattice deformation may be described by writing $F_p(\vec{R}_i-\vec{R}_j)\to F_p(\vec{R}_i,\vec{R}_j)=F_p^0(\vec{R}_i-\vec{R}_j)+\delta F_p(\vec{R}_i,\vec{R}_j)$ and $G(\vec{R}_i-\vec{R}_j)\to G(\vec{R}_i,\vec{R}_j)=G^0(\vec{R}_i-\vec{R}_j)+\delta G(\vec{R}_i,\vec{R}_j)$ in Eq. (31), where F_p^0 and G^0 are the couplings between electron lattice sites in some perfect reference lattice. One then may treat δF_p and δG as perturbations in precisely the same manner as we treated ΔU_i above. The resulting depletion $D(j)$ has precisely the same form as

in Eq. (36), with the only difference being that the matrix appearing in the definition of $\langle k|\Delta U|j\rangle$ now has off-diagonal matrix elements due to δF_p and δG. The resulting expression for the depletion of the lowest collective mode $D(0)$ has the same form as Eq. (39), although the precise form of $|\Delta U(q)|^2$ will be more complicated than for the diagonal disorder model. The important point, however, is that the energy denominators in the perturbation theory will be unaffected, so that one still expects only a weak logarithmic divergence if the disorder is not too strong, and a resulting sharp electromagnetic absorption for a finite size system. This demonstrates, albeit *a posteriori*, that our assumption of a diagonal disorder model does not alter the qualitative physics of the system, at least for weak disorder.

As is clear from the above discussion, the precise results for the length scale L_c depend upon the disorder model one uses for $\Delta U(\vec{q})$. In the next section, we introduce a simple model for this due to imperfections in the interface upon which the 2DEG resides.

IV. INTERFACE PINNING MODEL

In both the QHA and the perturbative analysis described above, one must make a specific choice for the (disorder) pinning potential. In Sec. V we present results for three different models. The first is a simple white-noise type model, in which some fixed fraction of the electrons are given an excitation energy $v_0+\Delta U_i=U_p$ between the $m=0$ and $m=1$ orbital states, and all other sites are unpinned. The simplicity of this model allows a clear comparison of results obtained from the QHA and the perturbative analysis. A second model we investigate is based on the idea that charged impurities are likely to be present in the spacer layers of heterojunction systems, and that some of these impurities, if close enough to the 2DEG, will substitute for electrons in the lattice.[26] By choosing a small number of lattice sites to have extremely large values of U_p, we can model this type of disorder within the QHA. As will be seen, this leads to a band of collective excitations well above the phonon band, corresponding to localized excitations of the strongly pinned electrons. At low excitation frequencies, these electrons are essentially immobile, and so behave as if they were not degrees of freedom. This is by definition a strongly pinned system; yet we will see in Sec. V that the resulting pinning frequency is extremely small, and that an unacceptably large number of such charged impurities must be present in the system to account for the experimentally observed magnitude of the pinning frequency.

We thus focus on a pinning mechanism which, to our knowledge, has not been previously discussed in the context of the magnetically induced WC: interface disorder. The interfaces between GaAs and AlAs at which the 2DEG's reside are by design of very high quality in samples such as those of Refs. 15 and 16. Nevertheless, they cannot be perfect, and it is generally accepted[28] that such interfaces can only be defined to within a single lattice constant of the host semiconductors. A simple idealization of this is to model the interface as a series of pits and/or terraces, with the height of the interface fluctuating randomly up and down as illustrated in Fig. 5. The typical scale of the pits and terraces formed by the imperfect interface is generally thought[28] to be of the order of several tens of angstroms. For the hole samples of Refs. 15 and 16, the interface has an additional corrugated structure with a size scale of 32 Å and a depth of 10.2 Å.[17,41]

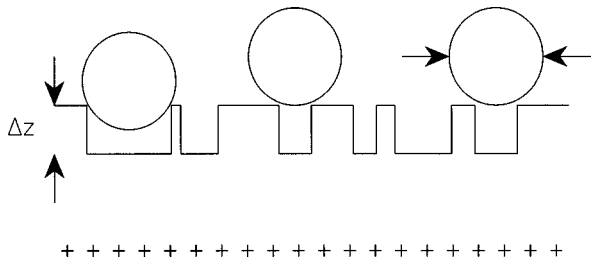

FIG. 5. Schematic representation of the interface disorder model. The interface has pits and terraces so that the setback from the ionized donor plane varies by a distance of order Δz. Electrons localized by the magnetic field into wave packets in the x-y plane of size scale $\sim l_0$ may lower their energy by moving their centers close to pit centers, since in the area of the pit the electron will be closer to the donor layer. For larger pits or decreasing magnetic length, more of the electron wave packet overlaps with the pit region, decreasing the energy of the wave packet.

There are several reasons for believing that this form of disorder may be important in the experiments of Refs. 15 and 16. First, the magnetic field at which one first sees a clear resonance at the lowest available temperatures is roughly 8 T, corresponding to a magnetic length of $l_0\sim 90$ Å, a very reasonable length scale below which one might expect the interface structure to trap electrons. If we model the pits in the interface as flat depressions of depth Δz as in Fig. 5, one can estimate the trap potential for a large pit by assuming the electric field between the 2DEG and the charged remote donors is uniform.[42] In this case the the potential gained from placing an electron in a pit that is much larger than the magnetic length is $\Delta V=2\pi\rho_0 e^2\Delta z/\kappa\approx 4.35$ K in temperature units; $\kappa\approx 12$ here is the dielectric constant of the GaAs host for the electrons, and we have taken $\Delta z=10$ Å. It should be noted that for experimentally accessible magnetic fields, a typical pit size will generally be much smaller than the magnetic length, so that the pinning energy of an electron trapped in a single pit will be of order $\Delta V s^2/l_0^2$, considerably smaller than the maximum possible value of ΔV.

Because of the roughness of the interface, the WC in general will distort slightly so that some or all of the electrons may take advantage of the interface potential. Ultimately some fraction of the electrons will find equilibrium centers for their (ground state $m=0$) Gaussian orbitals that are particularly low in energy. Because the first excited ($m=1$) state of each orbital is spatially far from the center of the $m=0$ state (in the sense that l_0 is larger than the average pit size s_0), the former state will not be correlated with the disorder potential, and thus is not on average lowered in energy as is the $m=0$ state. It should also be kept in mind that for a given ground state configuration, the energy of an excitation of a *single* electron from the $m=0$ state to the $m=1$ state, keeping all the other electrons fixed, will have its largest contribution from the electron-electron interaction rather than from the interface disorder. Provided the disorder is not too strong, the potential well in which an individual electron resides is thus to a first approximation circularly symmetric, so that the expansion in terms of angular momen-

tum states used in this work is sensible.

To fully specify the interface disorder model, we need to find the energy due to the disorder to excite an electron out of its ground state orbital ($m=0$) into the lowest excited state ($m=1$) for each site i, $\varepsilon_i(m=1)-\varepsilon_i(m=0)=v_0+\Delta U_i$. The distribution of ΔU_i depends upon the assumptions one makes about the surface morphology of the interface, as well as whether other pinning sources besides interface roughness are present in the system. We plan to make a fuller accounting of various possible models in the future;[43] here we will focus on one reasonable possibility that reproduces both the magnetic field and density dependence of the resonance frequency observed in the experiments of Ref. 15.

In this model we make the plausible assumption that the strongest pinning in the hole samples comes from defects and disorder in the interface corrugations of these systems. (It may be shown that perfectly regular corrugations of this sort lead only to very weak pinning.[43]) As a simple model of this, we assume that the surface has pits of size scale $s_0=30$ Å and depth $\Delta z=10$ Å with a surface density n_i. We will assume the average distance between pits $1/\sqrt{n_i}$ is smaller than the nearest neighbor separation of the electrons a but larger than the magnetic length l_0. This means that each unit cell of the WC contains several pits in which an electron might be trapped, but when trapped an electron wave packet covers one and only one pit. In what follows we will choose the density n_i to fit the experimental data at the lowest fields for which a resonance is observed; we then need to go back and check that the resulting pit density is consistent with $l_0<1/\sqrt{n_i}<a$.

To estimate the density of pinned electrons, we use the collective pinning approach that has been very successful in the context of vortices in superconductors[44] and charge density waves.[7,13] The basic idea is to find a size scale R_c of correlated domains, whose positions may adjust more or less independently of one another to take advantage of the pinning potential, at the expense of lattice distortion energy. The average number of pins that may be found under electron wave packets in a single domain if placed at a random location is given by $N_{\rm pin}=\rho_0 R_c^2 \pi l_0^2 n_i$; if we vary the position of the domain a distance of the order of the disorder correlation length (in this case, $1/\sqrt{n_i}$), one expects fluctuations in the number of pinned electrons of order $\sqrt{N_{\rm pin}}$. Since the energy gained by an electron wave packet when sitting over a pit is $\Delta V s_0^2/l_0^2$, in analogy with the Fukuyama-Lee-Rice (FLR) model for charge density waves, the energy per electron gained from the disorder potential $u_p^{\rm FLR}$ is

$$u_p^{\rm FLR}\approx \Delta V \frac{s_0^2}{l_0 R_c}\left[\frac{\pi n_i}{\rho_0}\right]^{1/2}.$$

The introduction of such distortions inevitably leads to a lattice distortion of amplitude $1/\sqrt{n_i}$ over a distance R_c. Following Ref. 13, we assume the distortions are purely transverse, and so estimate the distortion energy per electron to be

$$u_d^{\rm FLR}\approx \frac{\mu}{n_i R_c^2 \rho_0},$$

where μ is the shear modulus of the lattice. Minimizing the total energy $u_d^{\rm FLR}-u_p^{\rm FLR}$ with respect to R_c, we arrive at the optimum domain size

$$R_c=\frac{2\mu l_0}{\Delta V s_0^2(\pi n_i^3 \rho_0)^{1/2}}. \tag{42}$$

The resulting pinning energy per particle is found by substituting this value of R_c into our expression for $u_p^{\rm FLR}$, leading to the expression

$$u_p^{\rm FLR}\approx \frac{\pi \Delta V^2 s_0^4 n_i^2}{2\mu l_0^2}.$$

To use this, we need an explicit form for the shear modulus. This can be deduced from the transverse phonon dispersion relation of the WC in the absence of a magnetic field, which has the form $\omega_T(q)^2=(\mu/m^*\rho_0)\,q^2$, where m^* is the electron effective mass. The transverse mode eigenfrequency has been shown[38] in the classical harmonic approximation to be given approximately by

$$\omega_T(q)^2=0.036\omega_p^2(aq)^2,$$

with $\omega_p^2=4\pi e^2/\sqrt{3}m^*\kappa a^3$. Using the above equation, one arrives at the estimate

$$\mu\approx 0.3\frac{e^2}{\kappa a^3}. \tag{43}$$

The resulting pinning energy per particle is finally given by

$$u_p^{\rm FLR}\approx 5.24\frac{\kappa a^3 \Delta V^2 s_0^4 n_i^2}{e^2 l_0^2}. \tag{44}$$

In the perturbative regime, where the effective depth of the individual pinning centers, $\Delta V s_0^2/l_0^2$, is much smaller than the bandwidth of the phonon density of states, the pinning frequency is just given by the average binding energy per site, so that one finds $\omega_{\rm pin}\approx v_0\approx u_p^{\rm FLR}$, with $u_p^{\rm FLR}$ given by Eq. (44). Note within this approximation, $\omega_{\rm pin}\propto l_0^{-2}\propto B$, which leads to a pinning frequency that *increases* with magnetic field, as seen in experiment. It is also interesting to note that $\omega_{\rm pin}\propto a^3\propto 1/\rho_0^{3/2}$, which is also consistent with experimental results.[45] We will obtain quantitative estimates for v_0 in the next section using the above expressions.

When the pinning potential for an electron trapped by a pit approaches the bandwidth of the phonon density of states, the perturbative estimate above becomes quantitatively inaccurate, and one needs to perform a QHA calculation to obtain reliable results for $\omega_{\rm pin}$. To do this, we need the probability that a given electron will be trapped in a pit, which in this approach is given by $u_p^{\rm FLR}/\Delta V(s_0^2/l_0^2)$. We are then led to consider a distribution of pinning energies in which most electrons are unpinned, and a small fraction are pinned with an effective potential $v_0+\Delta U_i=\Delta V s_0^2/l_0^2$. The resulting model is then formally identical to the white-noise model mentioned above.

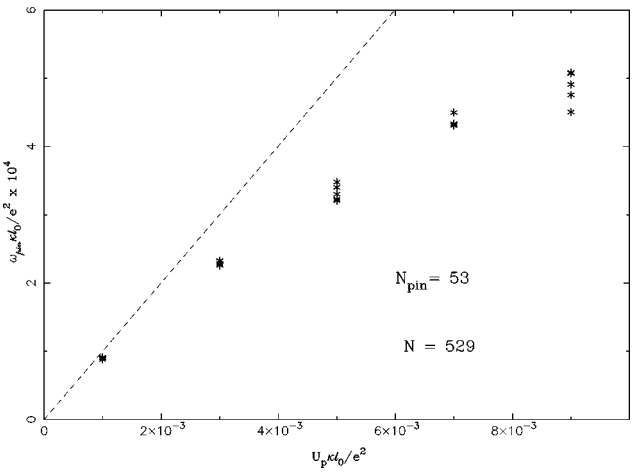

FIG. 6. Pinning frequency $\omega_{\rm pin}$ for a system of $N=529$ electrons, at filling fraction $\nu=0.2$, as a function of the pit potential. 10% of the electrons are pinned at random sites with energy $\Delta U=U_p$; the remaining electrons are unpinned. Stars are the results of the QHA for five different disorder realizations at each value of U_p, with two states per site retained in each calculation. Dotted line is the expected pinning frequency as calculated in lowest-order perturbation theory. For small values of U_p the approaches agree quite well; for larger values the perturbation theory sets an upper bound on the pinning frequency.

V. RESULTS

In this section we describe in more detail the results of our study. As has been emphasized, the electromagnetic responses computed in the QHA in all the models we have studied are qualitatively the same: one finds a single sharp line dominating the absorption spectrum. This line is very robust in that its weight shows no discernible decrease with increasing system size, and for models in which the pinning potential of the individual electrons is small compared to the width of the phonon density of states (Fig. 4), the frequency of the resonance occurs at the average excitation energy per electron, as expected from the perturbative analysis of Sec. III. We begin by describing in more detail the results for disorder that is in this sense weak.

A. Pinning by weak disorder

A particularly useful model for comparison of the QHA and perturbative analysis is one in which a fixed fraction $n_{\rm pin}=N_{\rm pin}/N$ of randomly chosen electrons is pinned, with each such site assigned the same pinning potential $v_0+\Delta U_i=U_p$. According to the perturbative analysis, the pinning frequency $\omega_{\rm pin}\approx n_{\rm pin}U_p$, regardless of the precise distribution of pinned sites. Figures 1 and 2 show typical results for this model, with half the sites pinned, using $U_p=0.01e^2/\kappa l_0$. Figure 6 illustrates the values of $\omega_{\rm pin}$ as computed in the QHA for five different disorder realizations each at several different values of $v_0+\Delta U_i=U_p$, for a smaller density of pinned sites (10%), and $\Delta U_i=0$ for all other sites, along with the prediction of the perturbative analysis (dotted line). For small U_p the agreement of the two approaches is quite good. Furthermore, there is almost no variation in $\omega_{\rm pin}$ for a fixed value of U_p when it is small as the precise realization of the pinned sites is changed. The interpretation of this observation is that, for small U_p, $\omega_{\rm pin}$ is determined almost exclusively by the restoring force on the WC when only the center of mass coordinate is moved with the lattice itself undistorted. Lattice distortions do introduce some deviation in the resonance frequency, generally pushing it below the value expected from the lowest-order perturbation theory, in a way that *does* depend on the precise disorder realization as may be seen in the figure. However, for any given disorder realization, a single mode always dominates the response; broadening is never observed for a fixed disorder configuration.

We note that with higher-order corrections to the perturbation theory of Sec. III, more accurate predictions of $\omega_{\rm pin}$ can be made for a given disorder realization. For example, one of the configurations in Fig. 6 with $U_p=0.003$ has $\omega_{\rm pin}=2.32\times10^{-4}$. (The numbers for both $\omega_{\rm pin}$ and U_p here are in units of $e^2/\kappa l_0$.) The lowest-order perturbation theory predicts $\omega_{\rm pin}\approx\omega_{\rm pin}^{(0)}=3\times10^{-4}$ at this density of pinning sites, which is in error by approximately 35%. Using the methods of Sec. III, the second-order correction may be computed for this particular disorder realization, with the result $\omega_{\rm pin}\approx\omega_{\rm pin}^{(0)}+\omega_{\rm pin}^{(2)}=2.19\times10^{-4}$, which is within 5.6% of the QHA result, a considerable improvement. (Note that the first order correction in ΔU_i, $\omega_{\rm pin}^{(1)}$, precisely vanishes in our perturbative approach.) Another significant point, as stated above, is that the weight of this single mode shows remarkably little size dependence. For example, using the parameters relevant to Fig. 1, the power absorption per electron at the frequency of the sharp peak in the inset of Fig. 1 is proportional to $\chi_{xx}(\omega_{\rm pin})\omega_{\rm pin}/N=0.006\,209$, where $N=1024$ for this calculation. For precisely the same system parameters, but $N=529$, one finds $\chi_{xx}(\omega_{\rm pin})\omega_{\rm pin}/N=0.006\,200$, a slight *decrease* for the smaller system size. This decrease is almost certainly related to the fact that the disorder realizations in the two calculations are inevitably different, rather than to any systematic increase with increasing system size. Nevertheless, this result illustrates that one cannot discern a decreasing weight in the sharp response with increasing system size for the values of N one may handle in the QHA.

The important question remains: to what extent, and under what conditions, does this response remain sharp for systems of experimentally relevant sizes? To address this question, we turn to the perturbative treatment of Sec. III. It was shown there that it is convenient to compute the power absorption by starting from a uniformly pinned state — i.e., a pinning potential that is the same for all electrons in the system — and computing perturbatively the corrections to this absorption spectrum due to the fact that the pinning potential is not truly uniform. For the uniformly pinned system, it is not at all surprising that energy absorption from a spatially homogeneous (time-dependent) electric field is dominated by a single mode: the collective modes have a well-defined wave vector $\vec{k}$, and only the $\vec{k}=0$ mode can couple to the electric field. In principle this $\vec{k}=0$ mode is mixed in among all the modes when disorder is introduced. Thus, as discussed more carefully in Sec. III, we are led to ask whether there is a finite overlap between the $\vec{k}=0$ collective

mode for the uniformly pinned case and the lowest-frequency collective mode in a disordered system in the thermodynamic limit.

In Sec. III we showed that this overlap may be written in the form $1-D$, with D given to second order in perturbation theory by

$$D=\frac{1}{\rho_0}\int\frac{d^2q}{2\pi}\left\{\frac{|u_{\vec{q}}^{+}|^2|\Delta U(\vec{q})|^2}{[v_0-E_q^p]^2}+\frac{|u_{\vec{q}}^{-}|^2|\Delta U(\vec{q})|^2}{[v_0+E_q^p]^2}\right\}, \tag{45}$$

with $\Delta U(\vec{q})=(1/\sqrt{N})\,\Sigma_i \Delta U_i e^{i\vec{q}\cdot\vec{R}_i}$, and ΔU_i is the deviation of site i from the site-averaged value of the pinning potential, v_0. Explicit expressions for $u_{\vec{q}}^{+}$ and $u_{\vec{q}}^{-}$ are given in Eqs. (37) and (38), and E_q^p is the dispersion relation for the uniformly pinned system, Eq. (24). For small q, as shown above [Eq. (28)]

$$E_q^p \approx v_0+2\pi e^2 l_0^2\rho_0 q+O(q^2),$$

so that D diverges in the thermodynamic limit, if $|\Delta U(\vec{q})|^2 \to \overline{|\Delta U|^2}>0$ as $q\to 0$, as is typically the case for white-noise potentials such as the one studied here. The meaning of this divergence is that essentially all the weight of the $\vec{q}=0$ mode for the uniformly pinned system has been depleted by the disorder from the lowest-energy collective mode, and is distributed among the other collective modes. However, in practice D is only divergent in the thermodynamic limit, since the integral in Eq. (45) has an infrared cutoff $q_{\min}=2\pi/L$, where L is the linear dimension of the system size. The depletion becomes significant ($D\approx 1$) for system sizes $L>L_c$, which in Sec. III was found to be [Eq. (41)]

$$L_c \approx \ell \exp\left\{\frac{\nu^3}{|\Delta\tilde{U}|^2}\right\}, \tag{46}$$

where $|\Delta\tilde{U}|^2$ is the disorder-averaged square potential evaluated in units of $e^2/\kappa l_0$ for $q\to 0$, and $2\pi/\ell$ is a wave vector below which the small q expansion for the uniformly pinned collective mode spectrum [Eq. (27)] becomes reasonably accurate; presumably $\ell \approx 10 a_0$, with a_0 the interelectron lattice spacing.

For system sizes $L\ll L_c$, the depletion remains small, so that a single sharp resonance should still be present. This means that one may interpret L_c as a length scale for which the electrons in an infinite sample move together coherently. To estimate the width of the resulting resonance, we note that the fluctuations in the pinning potential averaged over a length scale of L_c will be $n_{\rm pin}[1\pm a_0/L_c](\overline{\Delta U^2})^{1/2}$, so that the effective Q of the resonance would be $L_c/2a_0$. If L_c is very large, clearly this leads to an extremely narrow resonance. In fact, even a conservative estimate of L_c shows that it is larger than the physical dimensions of any real sample. Taking $(\overline{\Delta U^2})^{1/2}\approx 10\omega_{\rm pin}$, so that $\Delta\tilde{U}\approx 10\omega_{\rm pin}\kappa l_0/e^2 \approx 0.014$, where $\omega_{\rm pin}$ is the observed[15,16] resonance frequency of 1.25 GHz, and we used a magnetic length $l_0\approx 81$ Å appropriate for a 10 T magnetic field. (We expect that $|\Delta\tilde{U}|$ is considerably smaller than this.) At this field, the filling factor for the experimental densities is $\nu=0.22$, so that $L_c \sim 10^{24} a_0$, far larger than any real sample. The conclusion then is that $L_c \gg L$ in Refs. 15 and 16, and the electrons at zero temperature react essentially as a single domain in response to the (spatially uniform) electric field. Furthermore, the depletion D is in fact small in spite of the formal divergence when $L\to\infty$ at second order in perturbation theory; this accounts for the sharpness of the measured response at the lowest temperatures.[15,16]

Finally, it must be emphasized that this effect arises purely due to the long-range nature of the Coulomb interaction. For short-range potentials, $E_q^p - v_0 \sim q^2$, and the divergence in Eq. (45) is much stronger. This observation leads to another interpretation of the result: for short-range interactions, the phonon density of states for a uniformly pinned system at small frequencies is much larger than is the case for long-range interactions. (In the former case the phonon density of states jumps at the band edge, whereas in the latter it rises linearly from zero.) Thus, if one displaces the center of mass of the system (i.e., creates a $q=0$ excitation), for Coulomb interactions there are very few states into which the disorder can scatter this excitation. The calculations in this work demonstrate that the suppression of the phonon density of states at the band edge by the Coulomb interaction is sufficiently strong to leave a finite oscillator strength of the pure center of mass ($q=0$) mode in the lowest-frequency collective mode when disorder is included.

The observation that Coulomb interactions are crucial to getting the sharp response is consistent with the results of the QHA: Fig. 2 illustrates response for a single disorder realization when the Coulomb interaction is screened. For this calculation, we took an electron-electron interaction of the form

$$v(\vec{q})=2\pi e^2/\kappa\sqrt{q^2+q_c^2},$$

with $q_c=2.0 l_0^{-1}$, $N=225$, and the parameters are otherwise the same as for Fig. 1. The broadening even for this relatively small system is already apparent.

B. Pinning by charged impurities

A commonly accepted model for understanding the magnitude of the depinning threshold observed in dc voltage-current measurements[4,12,46] is one in which charged impurities close to the 2DEG become incorporated in the lattice as substitutions for electrons.[26] This is a paradigm for a strongly pinned system,[7] where certain locations of the lattice are essentially ''nailed down,'' and eliminated as degrees of freedom. In CDW systems, the pinning frequency for this type of disorder is estimated as the frequency of a phonon mode for the pure system, evaluated at wavelength $q\sim 2\pi/d$, where d is a typical separation between pinned sites. Using the QHA, we can quantitatively investigate this model to test whether it can account for the ~ 1 GHz resonance as well.

The method for emulating the charged impurity model within the QHA is to choose a small number of sites for which ΔU_i is larger than the width of the phonon density of states. A typical collective mode density of states arising from this type of disorder realization is illustrated in Fig. 7. Two peaks emerge, one at high frequency above the resonance frequency of the individual pinned sites, the other

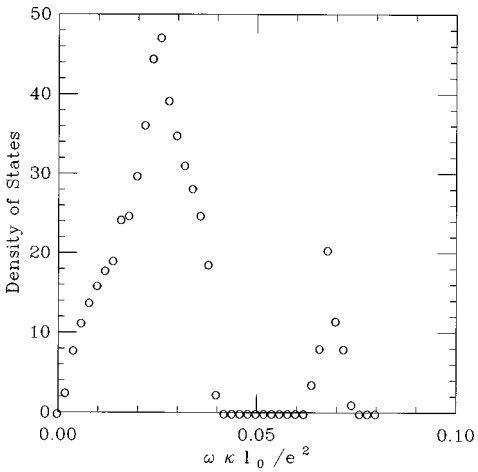

FIG. 7. Density of states for a strongly pinned WC, computed using the QHA, with $N=529$, $\nu=0.2$, and two states retained per site. 10% of sites have a pinning potential $v_0+\Delta U_i=U_p=0.04e^2/\kappa l_0$, a relatively large pinning potential; the rest are unpinned. A high-energy set of collective modes may clearly be seen separated above the main peak. These modes arise due to localized collective modes of the strongly pinned electrons. For the modes in the lower, main peak, the pinned electrons are essentially stationary.

shifted slightly upward from the phonon density of states for the pure system. It is easily checked that the motion of the electrons in the lowest-energy modes leaves the pinned electrons stationary, so that the magnitude of the pinning potential on these sites is irrelevant for these modes; in practice these electrons are removed as degrees of freedom.

Figure 8 illustrates the frequency of the lowest collective mode as a function of pinned site density, with several different disorder realizations. As in all the results of this work, the electromagnetic absorption is dominated for each realization by only the lowest mode.[47] At low densities, the frequency is approximately linear in the pinning site density, a

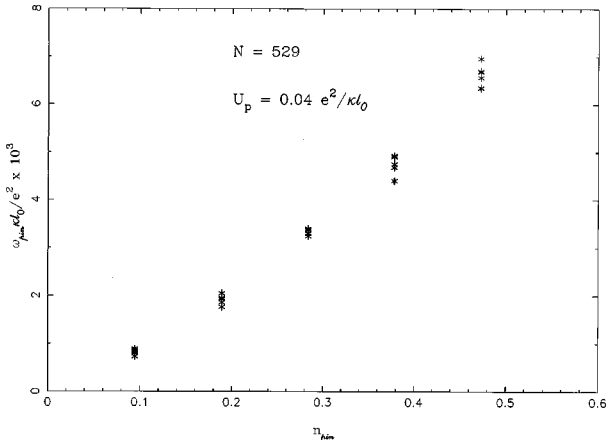

FIG. 8. Pinning frequency $\omega_{\rm pin}$ for a system of $N=529$ electrons with strong pinning centers. $\omega_{\rm pin}$ was computed using the QHA with two states per site at filling fraction $\nu=0.2$ as a function of $n_{\rm pin}$, the fraction of pinned sites, with $v_0+\Delta U_i=U_p=0.04e^2/\kappa l_0$ the potential of the pinned sites. ($1-n_{\rm pin}$ of the sites are unpinned.) Stars are the results for five different disorder realizations at each value of $n_{\rm pin}$. The computed frequencies are significantly lower than what is expected from an estimate based on strong pinning of an elastic medium.

result quite reminiscent of what was found for the weak pinning model of Sec. V A. The magnitude of the pinning frequencies found is surprisingly small; if one extrapolates the linear behavior for small pinning densities, we find that $\sim 13\%$ of the sites would have to be pinned in order to achieve the 1.25 GHz resonance seen at $\nu=0.2$. Such a high density of charged impurity substitutions near the 2DEG is clearly inconsistent with the high mobilities these samples exhibit in zero magnetic field. Furthermore, the pinning frequency is a monotonically decreasing function of field in this model, contrary to experimental observation. It thus seems quite clear that this model cannot be the primary pinning source relevant in electromagnetic absorption.

The behavior of the pinning mode at low impurity densities is surprising in its similarity to the results of the weak pinning model above, given that this is intrinsically a strong pinning mechanism. Indeed, the results of a strongly pinned CDW estimate grossly overestimate the pinning frequency at the densities we have studied. For example, if we assume a pinned site fraction $n_{\rm pin}=0.05$, then for filling factor $\nu=0.2$ the strong pinning estimate yields an expected pinning frequency greater than $7\times10^{-3}e^2/\kappa l_0$, while the frequency found in the QHA is roughly $5\times10^{-4}e^2/\kappa l_0$. This great disparity between the strongly pinned CDW estimate and the result of a more realistic calculation we believe exemplifies the limits of using CDW theory to quantitatively analyze properties of the magnetically induced WC. Indeed, we believe the tendency for the system at low $n_{\rm pin}$ to behave so much like a weakly pinned WC may be understood if one thinks of a strongly pinned electron as a charged impurity to which a vacancy in the WC has become bound. One then may think of the strongly pinned WC as a weakly pinned WC with point defects, and it is likely that a perturbative analysis of this system as in Sec. III would explain the sharpness of the response found from the QHA. If so, the strongly pinned WC for the purposes of ac response is equivalent to a weakly pinned, defective WC.

C. Interface pinning model

We now turn to the results of the interface pinning model defined in Sec. IV. As a first estimate, we use the perturbative result $\omega_{\rm pin}\approx v_0\approx u_p^{\rm FLR}$, with $u_p^{\rm FLR}$ given by Eq. (44). As discussed in Sec. IV, we set $s_0=30$ Å, $\Delta V=4.3K\approx 90$ GHz, and take $a=480$ Å, and $\kappa=12$, as is appropriate for the experiments of Ref. 15. To estimate the density of pits n_i, we set $v_0=u_p^{\rm FLR}\approx 1$ GHz at $B=8$ T,[15] for which $l_0\approx 90$Å, and use Eq. (44) to solve for n_i; the result is $n_i\approx 2.5\times10^{11}$ cm^{-2}. The resulting average distance between pits is $1/\sqrt{n_i}\approx 200$ Å, which clearly falls into the range of validity of our model, $l_0<1/\sqrt{n_i}<a$. We note with this estimate of n_i, the (Fukuyama-Lee-Rice) correlation length R_c with the use of Eqs. (42) and (43) is found to be $R_c\approx 7.5a$. Figure 9 illustrates the result of the perturbative estimate (solid line) as a function of magnetic field for this set of parameters.

The actual potential for sites that are pinned turns out to be large enough that the perturbative approach overestimates the value of $\omega_{\rm pin}$ noticeably. We thus turn to the QHA to get a more accurate estimate of the pinning frequency. As discussed above, this requires us to find the what fraction of electrons is pinned; for the above parameters, this works out

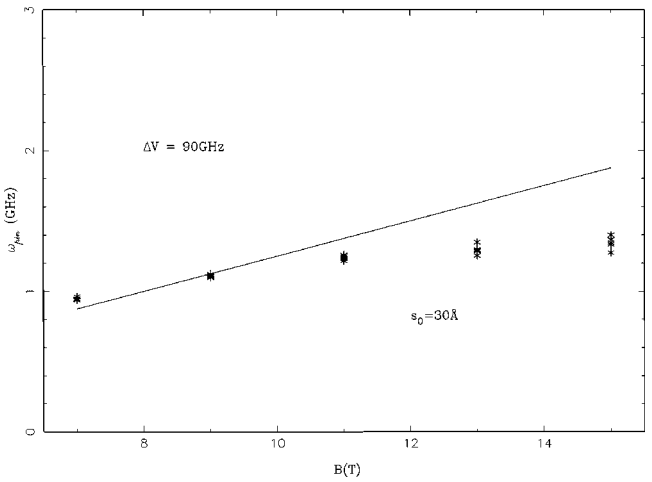

FIG. 9. Pinning frequency $\omega_{\rm pin}$ in the interface pinning model as a function of magnetic field, for $\Delta V = 90$ GHz corresponding to a pit depth of $\Delta z = 10$ Å. The average pit size $s_0 = 30$ Å, and the electron density in this figure is fixed at $\rho_0 = 5\times 10^{10}$ cm^{-2}. Solid line illustrates the perturbative estimate of $\omega_{\rm pin}$ for a pit density of $n_i = 2.5\times 10^{11}$cm^{-2}. The magnitude of the pinning frequency may be seen to increase linearly with magnetic field, due to the decreasing magnetic length of the Gaussian orbitals in which the electrons reside in the ground state. Stars represent the results of a quantum harmonic approximation (QHA) calculation with the same parameters except for a slightly increased pit density, $n_i = 3.0\times 10^{11}$cm^{-2}. Results for five different disorder realizations are shown for $B = 7$, 9, 11, 13, and 15 T.

to $n_{\rm pin} = N_{\rm pin}/N = u_p^{\rm FLR}/\Delta V(s_0^2/l_0^2) \approx 10\%$. It is interesting to note that, since $u_p^{\rm FLR} \propto l_0^{-2}$, the fraction of pinned electrons is independent of magnetic field. Each pinned electron has an excitation energy of $U_p = \Delta V s_0^2/l_0^2$ for these parameters. We can then proceed with the QHA precisely as in the calculations of Sec. V A. Using the parameters adopted for the perturbative approach, we find at $B = 8$ T in the QHA $\omega_{\rm pin} = 0.84$ GHz, slightly below the experimental value of 1 GHz. This indicates that we should raise our estimate of n_i, since its value was chosen to match the experimental result for this particular magnetic field. We find that the pinning frequency $\omega_{\rm pin} \approx 1$ GHz in the QHA if the fraction of pinned sites $n_{\rm pin}$ is raised to 11%; this can be achieved if we assume a pit density of $n_i = 3.0\times 10^{11}$ cm^{-2}. The results of this calculation are illustrated for several values of magnetic field in Fig. 9. As in Sec. V A, the perturbative result overestimates the pinning frequency by an increasingly large amount as the value of U_p at the pinned sites increases; this leads to the sublinear growth of $\omega_{\rm pin}$ with magnetic field that is apparent in the QHA result. It is interesting to note that experimentally the variation of $\omega_{\rm pin}$ with B is indeed found to be sublinear.[15]

VI. DISCUSSION

The primary result of this work, that the zero-temperature response of a pinned, magnetically induced two-dimensional WC to a spatially uniform, time-dependent electric field is sharp, to our knowledge is unanticipated in the literature. As we have seen, the key reason for this result is the long-range nature of the Coulomb potential. Early studies of a two-dimensional CDW system in a magnetic field[18] did note that for weak disorder potentials a calculation of the (static) CDW domain size diverges when a $1/r$ interaction is included. In Ref. 13 it was argued that this divergence may be removed by a careful treatment of the different energy scales for longitudinal and transverse distortions of the crystal. This treatment computed a lineshape for electromagnetic absorption by assuming the system may be thought of as independent Fukuyama-Lee-Rice domains, with randomness in the pinning frequencies of the individual domains satisfying $\Delta\omega_{\rm pin}/\omega_{\rm pin} \sim 1$. By noting that there must be a length scale over which the variations in domain pinning frequency effectively decouple the domains, an estimate for the expected line shape was found.

The model of Ref. 13 is in fact not very different than ours. One could think of the individual electrons in our calculations as FLR domains, and the model investigated would basically be the same. However, in that work it was assumed that the length scale over which Coulomb coupling may be ignored is the same as the FLR length, leading to a resonance with $Q \sim 1$. This reasoning works well in the absence of a magnetic field, because each domain has two possible polarizations for their motion in a collective mode. For the lowest frequency collective modes, the domains can execute a transverse motion that avoids long-range density fluctuations, which are very high in energy. Such long-range density fluctuations do appear when the motion of the domains is longitudinal, and so such modes contribute to the phonon density of states at high frequencies. For the transverse modes, the coupling of motion among the domains is weak, and the approximations of Ref. 13 make sense.

In the presence of a magnetic field, however, it is not possible to separate modes into transverse and longitudinal; these modes are inevitably mixed. The magnetic field causes the domains to move in a circular fashion, essentially circulating around their effective potential wells. However, if different domains circulate at different frequencies, there will necessarily be long-range density fluctuations, so that such modes will be high in energy. Low-frequency modes can be achieved if the coupling between domains is explicitly included, so that correlations in the motions of different domains may be introduced. This means in a magnetic field the system will have a *dynamical* correlation length that is different than the *static* (FLR) correlation length, and in this work we have seen that this dynamical correlation length is extremely large. We emphasize that this behavior is very different than what occurs in most CDW systems, where the static and dynamic correlation lengths are basically the same.[13,49] The new physics arises because of the unique combination of two dimensions, the long-range Coulomb interaction, and a magnetic field, and leads to the sharp resonance found in this work.

Experimentally, it is somewhat surprising that only the most recent measurements have uncovered the sharpness of this resonance, whereas there have been a number of earlier measurements of rf, surface acoustic wave, and microwave responses in this system[8–10,12] which found broad resonances. There may be several reasons for this. First, in order to couple to the 2DEG, the experimental methods probe the system at a finite $\vec{k}$, not with a purely spatially uniform electric field. From a practical viewpoint this is necessary, as the oscillator strength for transitions at small $\vec{k}$ is very small,

making detection of the absorbed energy difficult. However, a repetition of the analysis of Sec. III shows that the absorption is sharp *only* for $k=0$: the second-order correction in perturbation theory diverges more strongly at finite k than for $k=0$, indicating that the response broadens as k increases. This observation is supported by the results of Ref. 16, for which several absorption peaks are observed, presumably representing harmonics of the fundamental probing wavelength. The widths of these peaks are found to increase with increasing frequency. Thus it may be that some of the methods used in previous work coupled to or mixed in large enough values of k to wash out the resonance.

A second important aspect of the result is that it applies only at zero temperature; clearly one expects thermal broadening of the resonance, which we have not addressed in this work. This means that one can only expect such sharp resonances at the lowest temperatures. One study of the temperature dependence of the resonance[16] indicates that it is only apparent below 100 mK, and that it sharpens very rapidly in the range 50 mK$\rightarrow$30 mK. It seems quite reasonable that thermal broadening is responsible for the absence of this sharp resonance in previous experiments, especially since the temperature below which the sharp resonance settles in may be sample specific.

A number of open questions remain unresolved by this work. First, because this is a zero-temperature study, we have not been able to understand the detailed absorption line shape of Refs. 15 and 16. Beyond thermal effects, the large scale coherence of the electron motion at zero temperature indicates that specific dissipation mechanisms — in particular, edge states[17,48] — of the WC may prove important in this context. Beyond the lineshape, some aspects of the magnetic field dependence of the resonance remain unexplained: at the highest magnetic fields, the resonance shows little or no field dependence, while the Q of the resonance continues to increase with field. This work gives a natural explanation for how the frequency may be an increasing function of field in an interface pinning model; however, it is not clear how one could obtain a field-independent resonance. Investigations of these issues are currently being pursued.

VII. SUMMARY

In this work, we studied the response of a two-dimensional Wigner crystal in a strong magnetic field to a spatially uniform, time-dependent electric field, at zero temperature, pinned by a disorder potential. An approach to computing the response functions of a localized electron system in the lowest Landau level was introduced, the quantum harmonic approximation. It was found that the response is sharp; i.e., there is a resonance that is *not* disorder broadened. For weak disorder, this effect was shown within perturbation theory to survive for macroscopically large samples, because of the emergence of an extremely large length scale L_c that represents the distance over which electrons oscillate together in the lowest excited state of the system. The fact that L_c is so very large was shown to result primarily from the long-range nature of the Coulomb interaction. A model of interface pinning was shown to reproduce both the magnitude and some aspects of the field dependence of the resonance as observed in experiment.

The author has become aware of a recent investigation[49] of the pinning properties of the magnetically induced WC. These authors are also able to explain the increase of the pinning frequency with increasing field observed in experiment. However, the work does not find the unbroadened resonance at zero temperature that is the focus of the present paper.

ACKNOWLEDGMENTS

The author is indebted to Professor Sankar Das Sarma for telling him of the results of Ref. 15, as well as for many useful discussions and encouragement through the course of this work. Lloyd Engel, Chichun Li, Chris Mellor, and Dan Tsui are gratefully acknowledged for making the results of their work available prior to publication. The author also thanks Steve Girvin for a useful discussion. This work was supported by NSF Grant No. DMR98-70681, and the Research Corporation.

APPENDIX: COMPUTATION OF INTERACTION MATRIX ELEMENTS

The interaction matrix elements $U^{ij}_{m_1m_2m_3m_4}$ can be greatly simplified by the use of the strict translational periodicity assumed in this work. In general, they may be written in the form

$$U^{ij}_{m_1m_2m_3m_4}=\int d^2r_1d^2r_2\int d^2q v(q)e^{-i\vec{q}\cdot(\vec{r_1}-\vec{r_2})}\phi^*_{m_1}(\vec{r}-\vec{R}_i)\times\phi_{m_2}(\vec{r}-\vec{R}_i)\phi^*_{m_3}(\vec{r}-\vec{R}_j)\phi_{m_4}(\vec{r}-\vec{R}_j),$$

where $\phi_m(\vec{r})$ is the mth angular momentum state centered around the origin. The quantity $v(q)$ is the Fourier transform of the electron-electron interaction, which for most of this work will take the form $2\pi e^2/q$. [To describe a screened Coulomb potential, one may take $v(q)=2\pi e^2/\sqrt{q^2+q_c^2}$. This was the form used in the calculations leading to Fig. 2.] Because we are imposing periodic boundary conditions, the interaction needs to be replaced with one that is periodic in a superlattice of unit cells, each with N electrons, whose positions inside each cell are identical. This is accomplished by making the replacements $\vec{q}\rightarrow\vec{G}$, $\int d^2q\rightarrow(1/v_c)\Sigma_{\vec{G}}$ in the above expression, where $\{\vec{G}\}$ are the reciprocal lattice vectors of the superlattice, and v_c is the supercell area. Making this replacement, and switching over to bra-ket notation, we have

$$U^{ij}_{m_1m_2m_3m_4}=\frac{1}{v_c}\sum_{\vec{G}} v(\vec{G})\langle m_1|e^{-i\vec{G}\cdot\vec{r}}|m_2\rangle\times\langle m_3|e^{i\vec{G}\cdot\vec{r}}|m_4\rangle e^{-i\vec{G}\cdot(\vec{R}_i-\vec{R}_j)}. \quad \text{(A1)}$$

Although for the unscreened Coulomb interaction $v(\vec{G})$ diverges for $\vec{G}=\vec{0}$, we may formally set it to zero if one includes the effects of a uniform neutralizing background. The matrix elements $\langle m_1|e^{-i\vec{G}\cdot\vec{r}}|m_2\rangle$ may be computed with some work analytically. The result is

$$\langle m_1|e^{-i\vec{G}\cdot\vec{r}}|m_2\rangle=\left[\frac{m_2!}{m_1!}\right]\left[\frac{(Gl_0)^2}{2}\right]^{(m_1-m_2)2}\times L_{m_2}^{m_1-m_2}\left(\frac{(Gl_0)^2}{2}\right)\times e^{i(m_2-m_1)\left(\theta_{\vec{G}}+\frac{\pi}{2}\right)-(Gl_0)^2/2}, \quad \text{(A2)}$$

for $m_1 \geqslant m_2$, where θ_G is the angle between the the vector $\vec{G}$ and the $\hat{x}$ axis, and $L_{m_2}^{m_1-m_2}$ is an associated Laguerre polynomial. The expression for $m_2 > m_1$ may be obtained using $\langle m_1|e^{-i\vec{G}\cdot\vec{r}}|m_2\rangle=\langle m_2|e^{-i(-\vec{G})\cdot\vec{r}}|m_1\rangle^*$. It is convenient to write this result in the form

$$\langle m_1|e^{-i\vec{G}\cdot\vec{r}}|m_2\rangle=e^{i(m_2-m_1)(\theta_{\vec{G}}+\pi/2)}F_{m_1m_2}(G),$$

with

$$F_{m_1m_2}(G)=\left[\frac{m_2!}{m_1!}\right]\left[\frac{(Gl_0)^2}{2}\right]^{(m_1-m_2)/2}\times L_{m_2}^{m_1-m_2}\left(\frac{(Gl_0)^2}{2}\right)e^{-Gl_0^2/2}$$

for $m_1 \geqslant m_2$. For $m_1 < m_2$, the expression for $F_{m_1m_2}(G)$ has the same form as above, only with the indices m_1, m_2 interchanged.

The interaction matrix element can now be written in the form

$$U^{ij}_{m_1m_2m_3m_4}=\frac{1}{v_c}\sum_{\vec{G}} v(\vec{G})e^{-i\vec{G}\cdot(\vec{R}_i-\vec{R}_j)}F_{m_1m_2}(G)F_{m_3m_4}(G)\times(-1)^{m_4-m_3}i^{|m_1-m_2|+|m_3-m_4|}\times e^{i[m_2-m_1+m_4-m_3]\theta_{\vec{G}}},$$

which is particularly convenient for calculations. For a given value of $\vec{R}_i-\vec{R}_j$ one in practice can include a very large number of reciprocal lattice vectors in the sum; for example, our calculations with $N=1024$ electrons include approximately 60 000 different values of $\vec{G}$ in the sum. Because we include so many of these, the QHA can accurately reflect what happens at length scales shorter than a magnetic length, allowing one to treat disorder potentials that vary on a short length scale. This is the advantage the QHA has over the method of Ref. 24, which is typically limited to several hundred values of $\vec{G}$.

In the text, we took advantage of the sum rule

$$\sum_l U'^{il}_{m_1m_200}\equiv\sum_l U^{il}_{m_1m_200}-U^{ii}_{m_1m_200}\propto\delta_{m_1m_2}, \quad \text{(A3)}$$

which we now demonstrate. We begin with the simple observation that

$$\sum_j e^{i\vec{G}\cdot\vec{R}_j}=N\sum_{\vec{g}}\delta_{\vec{g},\vec{G}},$$

where the $\{\vec{g}\}$ are the reciprocal lattice vectors of the electron lattice (i.e., not the superlattice). Then

$$\sum_l U^{il}_{m_1m_200}=N\sum_{\vec{g}} v(g)\langle m_1|e^{-i\vec{g}\cdot\vec{r}}|m_2\rangle\langle 0|e^{i\vec{g}\cdot\vec{r}}|0\rangle.$$

From Eq. (A2) it is clear that $\langle 0|e^{i\vec{g}\cdot\vec{r}}|0\rangle$ depends only on the magnitude of $\vec{g}$ and not its orientation, so that the orientation angle enters the sum above through $\langle m_1|e^{-i\vec{g}\cdot\vec{r}}|m_2\rangle \propto e^{i(m_2-m_1)\theta_{\vec{g}}}$. Since each reciprocal lattice vector has five others of the same magnitude oriented at angles that are integral multiples of $\pi/3$ away from $\theta_{\vec{g}}$, it follows that the phase factor will cause the above sum to vanish unless $m_1=m_2$. Thus

$$\sum_l U^{il}_{m_1m_200}\propto\delta_{m_1m_2}. \quad \text{(A4)}$$

Similarly, for $U^{ii}_{m_1m_200}$ we have

$$U^{ii}_{m_1m_200}=\sum_{\vec{G}} v(G)\langle m_1|e^{-i\vec{G}\cdot\vec{r}}|m_2\rangle\langle 0|e^{i\vec{G}\cdot\vec{r}}|0\rangle.$$

As above, the quantity entering the sum involves the orientation of $\vec{G}$ only through $e^{i(m_2-m_1)\theta_{\vec{G}}}$, so this sum must also vanish unless $m_1=m_2$. Together with Eq. (A4), this proves the sum rule Eq. (A3).

[1] E.P. Wigner, Phys. Rev. **46**, 1002 (1934).

[2] For a perspective on recent efforts of this sort, see H.A. Fertig, in *Perspectives in Quantum Hall Effects*, edited by S. Das Sarma and A. Pinczuk (Wiley, New York, 1997).

[3] H.W. Jiang, R.L. Willett, H. Störmer, D.C. Tsui, L.N. Pfeiffer, and K.W. West, Phys. Rev. Lett. **65**, 633 (1990).

[4] V.J. Goldman, M. Santos, M. Shayegan, and J.E. Cunningham, Phys. Rev. Lett. **65**, 2189 (1990).

[5] M.B. Santos, Y.W. Suen, M. Shayegan, Y.P. Li, L.W. Engel, and D.C. Tsui, Phys. Rev. Lett. **68**, 1188 (1992).

[6] G. Grüner, Rev. Mod. Phys. **60**, 1129 (1988).

[7] H. Fukuyama and P.A. Lee, Phys. Rev. B **17**, 535 (1978).

[8] E.Y. Andrei, G. Deville, D.C. Glattli, F.I.B. Williams, E. Paris, and B. Etienne, Phys. Rev. Lett. **60**, 2765 (1988).

[9] M.A. Paalanen, R.L. Willett, P.B. Littlewood, R.R. Ruel, K.W. West, L.N. Pfeiffer, and D.J. Bishop, Phys. Rev. B **45**, 11342 (1992).

[10] R.L. Willett, Surf. Sci. **305**, 76 (1994).

[11] Y.P. Li, D.C. Tsui, T. Sajoto, L.W. Engel, M. Santos, and M. Shayegan, Solid State Commun. **95**, 619 (1995); Y.P. Li, D.C. Tsui, L.W. Engel, M. Santos, T. Sajoto, and M. Shayegan, *ibid.* **96**, 379 (1995).

[12] D.C. Glattli, G. Deville, V. Duburcq, F.I.B. Williams, E. Paris, B. Etienne, and E.Y. Andrei, Surf. Sci. **229**, 344 (1990); F.I.B. Williams, P.A. Wright, R.G. Clark, E.Y. Andrei, G. Deville, D.C. Glattli, O. Probst, B. Etienne, C. Dorin, C.T. Foxon, and J.J. Harris, Phys. Rev. Lett. **66**, 3285 (1991).

[13] B.G.A. Normand, P.B. Littlewood, and A.J. Millis, Phys. Rev. B **46**, 3920 (1992).

[14] M. Ferconi and G. Vignale, Phys. Rev. B **48**, 2831 (1993).
[15] C.C. Li, L.W. Engel, D. Shahar, D.C. Tsui, and M. Shayegen, Phys. Rev. Lett. **79**, 1353 (1997).
[16] P.F. Hennigan, A. Beya, C.J. Mellor, R. Gaal, F.I.B. Williams, and M Henini (unpublished).
[17] L.W. Engel (private communication).
[18] H. Fukuyama and P.A. Lee, Phys. Rev. B **18**, 6245 (1978).
[19] The microscopic model adopted in this work is qualitatively similar to that of Ref. 14. That work, however, focused on the value of the pinning frequency and did not directly compute the electromagnetic response of the WC. We believe a computation of this quantity within the model of Ref. 14 would lead to a sharp density response, as found in this work.
[20] K. Maki and X. Zotos, Phys. Rev. B **28**, 4349 (1983).
[21] W. Kohn, Phys. Rev. **123**, 1242 (1961).
[22] D.R. Fredkin and N.R. Werthammer, Phys. Rev. A **138**, 1527 (1965).
[23] Once we have projected into the lowest Landau level, there is no distinction between the cases when the charged particles in the WC are electrons and when they are holes. For clarity we refer to them throughout the text as electrons, even though in many experiments (particularly Refs. 15 and 16) the carriers are in fact holes.
[24] R. Côté and A.H. MacDonald, Phys. Rev. Lett. **65**, 2662 (1990); Phys. Rev. B **44**, 8759 (1991).
[25] A similar model has been analyzed in the context of cyclotron resonance. See U. Merkt, Phys. Rev. Lett. **76**, 1134 (1996).
[26] I.M. Ruzin, S. Marianer, and B.I. Shklovskii, Phys. Rev. B **46**, 3999 (1992).
[27] It should be noted that although pinning via charged impurities as discussed in Ref. 26 is inconsistent with experimentally measured pinning frequencies, it may well be true that this mechanism sets the energy scale for the static electric field threshold found in experiments. The possibility that nonlinear *IV* characteristics and low-frequency ac response are dominated by different pinning mechanisms could explain the difficulties in reconciling the experimental measurements of these with a model that has a reasonable crystalline correlation length (Refs. 13 and 14).
[28] A. Ourmazd, D.W. Taylor, J. Cunningham, and C.W. Wu, Phys. Rev. Lett. **2**, 933 (1989); C. Warwick, W.Y. Jan, A. Ourmazd, and T.D. Harris, Appl. Phys. Lett. **56**, 2666 (1990).
[29] See, for example, James Leo and A.H. MacDonald, Phys. Rev. Lett. **64**, 817 (1990).
[30] M.C. Cha and H.A. Fertig, Phys. Rev. Lett. **73**, 870 (1994); Phys. Rev. B **50**, 14368 (1994).
[31] G. Mahan, *Many-Particle Physics* (Plenum Press, New York, 1990).
[32] Note that this is where the approximation of ignoring overlaps between states localized at different sites is introduced.
[33] One may be more careful and directly compute $\int d^2r \langle \vec{j}(\vec{r},\omega)\rangle \cdot \langle \vec{E}_{\rm ind}(\vec{r},\omega)\rangle$ to account for spatial correlations between the current and induced electric field for a given disorder realization. However, for the very sharp responses we find at zero temperature, this difference is purely academic. At finite temperature where the response is broadened, this latter approach is preferable, although it is likely that the long-range nature of the Coulomb interaction will make the spatial variations in $\langle \vec{E}_{\rm ind}\rangle$ quite weak.
[34] R. Côté and A.H. MacDonald, Surf. Sci. **263**, 187 (1992).
[35] H. Fukuyama, Solid State Commun. **17**, 1323 (1975).
[36] As usual, when representing spin waves in terms of bosonic degrees of freedom, one must keep in mind that the number of bosons per site is constrained to be no more than 1. Provided one is interested in states with very few spin waves (as is the case here), the constraint does not need to be enforced explicitly.
[37] T. Holstein and H. Primakoff, Phys. Rev. **58**, 1098 (1940).
[38] L. Bonsall and A.A. Maradudin, Phys. Rev. B **15**, 1959 (1977).
[39] These properties are easily understood if one recognizes that the matrix is precisely the same as the one that must be diagonalized to express the pseudospin-wave creation and annihilation operators in terms of the site boson operators b_i, $b_i^\dagger$.
[40] E. Merzbacher, *Quantum Mechanics* (Wiley, New York, 1970).
[41] R. Nötzel *et al.*, Phys. Rev. B **45**, 3507 (1992); R. Nötzel *et al.*, *ibid.* **47**, 1299 (1993).
[42] T. Ando, A. Fowler, and F. Stern, Rev. Mod. Phys. **54**, 437 (1982).
[43] H.A. Fertig (unpublished).
[44] A.I. Larkin and Yu. N. Ovchinikov, J. Low Temp. Phys. **34**, 409 (1979).
[45] C.C. Li *et al.* (unpublished).
[46] Y.P. Li, T. Sajoto, L.W. Engel, D.C. Tsui, and M. Shayegan, Phys. Rev. Lett. **67**, 1630 (1991).
[47] We expect for extremely large densities of pinned sites that one should observe a broadening of the absorption. However, the density required for this is too large to be of physical interest.
[48] R. Côté and H.A. Fertig, Phys. Rev. B **48**, 10955 (1993); H.A. Fertig and R. Côté, *ibid.* **48**, 2391 (1993).
[49] R. Chitra, T. Giamarchi, and P. Le Doussal, Phys. Rev. Lett. **80**, 3827 (1998).